

C-MYC INHIBITION ALLOWS EX VIVO EXPANSION OF MURINE AND HUMAN  
HEMATOPOIETIC STEM AND PROGENITOR CELLS



by  
Merve Aksöz

Submitted to Graduate School of Natural and Applied Sciences  
in Partial Fulfillment of the Requirements  
for the Degree of Master of Science in  
Biotechnology

Yeditepe University  
2016

C-MYC INHIBITION ALLOWS EX VIVO EXPANSION OF MURINE AND  
HUMAN HEMATOPOIETIC STEM AND PROGENITOR CELLS

APPROVED BY:

Assist. Prof. Dr. Fatih Kocabaş  
(Thesis Supervisor)



Prof. Dr. Gamze Torun Köse



Prof. Dr. Nesrin Özören



DATE OF APPROVAL: .... / .... / 2016

## ACKNOWLEDGEMENTS

First and foremost, I would like to express my special gratitude and thanks to my thesis advisor Dr. Fatih Kocabaş for his continuous support, motivation, and guidance throughout my study. I would like to thank you for encouraging my research and for allowing me to grow as an independent research scientist. I gained the most knowledge and skill here in the subject of hematopoiesis and pushed me to study further on this area.

I would like to thank Prof. Dr. Nesrin Özören and Prof. Dr. Gamze Torun Köse for separating their time to be on my thesis committee, revising my work and valuable comments on this thesis.

I also would like to thank to The Scientific and Technological Research Council of Turkey (TUBITAK) for supporting me with the graduate scholarship during my study through TÜBİTAK 1001 program [grant number 115S185]. My studies have also been funded by Co-Funded Brain Circulation Scheme by The Marie Curie Action COFUND of the 7<sup>th</sup> Framework Programme of the European Commission.

I thank my labmates in Yeditepe University Regenerative Biology Research Laboratory (YU-REG): Esra Albayrak, Dolay Damla Çelik, Pınar Çolakoğlu, Galip Servet Aslan, Dilek Turan, Semih Arbatlı, Doğan Yücel, Batuhan Kalkan, Merve Uslu, Pınar Siyah, Seyhan Genç for their friendship and support during my good and bad times, fun and scientific environment. This work would not have been extended without the assistance of many. I also appreciate to Burçin Asutay and Emrehan Tüysüz for their technical assistance in flow cytometry.

I also thank to my best friend Çise Kızılırmak for her valuable friendship, motivation and fun. I also thank you guys Berceste Balcı, Dehan Çömez, Rûveyda Saraçoğlu, Gönül Seyhan, Egemen Özkan for your continuous support, friendship and beautiful memories.

Finally, special thanks to my family. I thank to my father Haluk Aksöz, my mom Sibel Aksöz and my brother Berke Aksöz for their endless love, support and patience. Your prayer for me was what sustained me thus far, without it would not be possible to succeed.

## ABSTRACT

### **C-MYC INHIBITION ALLOWS *EX VIVO* EXPANSION OF MURINE AND HUMAN HEMATOPOIETIC STEM AND PROGENITOR CELLS**

We have previously shown that targeting HSC quiescence regulators not only leads to cell cycle entry but also induces HSC expansion. Intriguingly, an oncogene, c-myc, opposed to what has been expected following loss of function in bone marrow leads to accumulation of HSPCs up to 4 fold *in vivo*. Thus, transient inhibition of c-myc could provide a mean to expand HPSCs *ex vivo*. To this end, we have utilized c-myc inhibitor 10074-G5 along with several hematopoietic small molecules (HSMs), namely tauroursodeoxycholic acid (TUDCA),  $\alpha$ -Tocopherol and the i-NOS inhibitor L-NIL. 10074-G5 and tested HSMs led to about 2-fold increase in murine LSKCD34<sub>low</sub> compartment post 7 days of treatment. Increased HSPC proliferation was also evident by decreased murine HSPC content in G<sub>0</sub> phase of the cell cycle. Furthermore, we treated human umbilical cord blood (UCB) cells with different doses of c-myc inhibitor. Similar to other HSMs we tested, c-myc inhibition increased CD34<sup>+</sup> and CD133<sup>+</sup> HSPC cell content up to 2-fold compared to control. In addition, we found that c-myc inhibition suppresses proliferation kinetics of bone marrow derived mesenchymal stem cells but do not alter proliferation of adipose derived mesenchymal stem cells. These findings suggest that c-myc inhibitor 10074-G5 and HSMs TUDCA,  $\alpha$ -Tocopherol, and L-NIL are specific to induction of HSPCs proliferation. This could be further exploited to increase *ex vivo* HPSC expansion and eventually transplantation efficiency.

## ÖZET

### **C-MYC İNHİBİSYONUNUN FARE VE İNSAN HEMATOPOETİK KÖK HÜCRE/HÜCRE PROGENİTORLERİNİN *EX VIVO* ÇOĞALMASINI ARTTIRICI ETKİSİ**

Hematopoetik kök hücre (HKH) dormansi regülatörlerinin susturulması HKH'lerin sadece hücre döngülerine katılmalarını sağlamakla kalmaz aynı zamanda HKH'lerin çoğalmasını sağlamaktadır. İlgi çekici bir şekilde, bir onkogen olan c-myc geninin kemik iliğindeki fonksiyon kaybı beklenenin aksine hematopoetik kök hücre/hücre progenitorlerinin *in vivo*'da 4-kata kadar artmasına öncülük etmiştir. Bu bulgular, c-myc onkogeninin geçici inhibisyonu hematopoetik kök hücre/hücre progenitorlerinin *ex vivo*'da çoğalabilmesine olanak sağlayabileceğini düşündürmektedir. Bu amaçla, çalışmamızda hematopoetik küçük molekülleri olan c-myc inhibitörü 10074-G5 ve bununla beraber tauroursodeoxycholik asit (TUDCA),  $\alpha$ -Tocopherol, i-NOS inhibitörü L-NIL kullandık. Hematopoetik küçük moleküllerle yedi günlük muamele sonunda 10074-G5 ve diğer hematopoetik küçük moleküller LSKCD34<sup>low</sup> popülasyonunu yaklaşık 2 kata kadar arttırmıştır. Hücre döngüsünün Go fazında bulunan fare hematopoetik kök hücre/hücre progenitorlerinin azalması, artan proliferasyona kanıt niteliğinde olmuştur. Ayrıca, insan kordon kanı hücreleri c-myc inhibitörünün farklı dozlarıyla muamele edilmiştir. Denediğimiz diğer hematopoetik küçük moleküllere benzer olarak, c-myc inhibisyonu CD34+ ve CD133+ hematopoetik kök hücre/hücre progenitorlerini kontrole göre 2 kata kadar arttırmıştır. Bunun dışında c-myc inhibisyonu kemik iliği proliferasyonunu baskılamak, adipoz-kökenli mezenkimal kök hücrelerinin proliferasyon kinetiğini etkilememiştir. Çalışmalarımızın sonucu gösteriyor ki c-myc inhibitörü 10074-G5 ve  $\alpha$ -Tocopherol ve L-NIL hematopoetik kök hücre/hücre progenitorlerinin çoğalmasına spesifiktir. Bu bulgular sonraki dönemlerde hematopoetik kök hücre/hücre progenitorlerini çoğaltmak ve transplantasyon verimini arttırmak için kullanılabilir.

## TABLE OF CONTENTS

ACKNOWLEDGEMENTS.....	iii
ABSTRACT.....	iv
ÖZET .....	v
LIST OF FIGURES .....	viii
LIST OF TABLES.....	x
LIST OF SYMBOLS/ABBREVIATIONS.....	xii
1. INTRODUCTION.....	1
1.1. HEMATOPOIETIC STEM CELLS .....	1
1.2. EX VIVO HSC EXPANSION.....	3
1.3. C-MYC GENE.....	4
1.4. C-MYC TARGET GENES .....	5
1.5. SMALL MOLECULE TARGETED <i>EX VIVO</i> HSC EXPANSION.....	7
2. MATERIALS AND METHODS.....	10
2.1. MATERIALS AND ANIMAL INFORMATION .....	10
2.1. BONE MARROW COLLECTION & MAGNETIC LINEAGE DEPLETION...	10
2.3. HEMATOPOIETIC STEM CELL STAINING OF MURINE BONE MARROW CELLS AND FLOW CYTOMETRY ANALYSIS .....	11
2.4. CELL COUNTING AND IMAGING .....	12
2.5. UMBILICAL CORD BLOOD CELL ISOLATION .....	12
2.6. FLOW CYTOMETRY ANALYSIS OF HUMAN HSPCS .....	13
2.7. CELL CYCLE ANALYSIS OF MURINE LSK CELLS .....	13
2.8. APOPTOSIS ANALYSIS OF MURINE LSK CELLS .....	14
2.9. COLONY FORMATION UNIT (CFU) ASSAY .....	14
2.10. COMBINATORIAL HSM TREATMENTS .....	14
2.11. BONE MARROW-DERIVED MESENCHYMAL STEM CELL ISOLATION.	15
2.12. ADIPOSE-DERIVED MESENCHYMAL STEM CELL ISOLATION .....	15
2.13. WST1 ANALYSIS.....	16
2.14. EFFECT OF HSM ON HUVEC .....	16

2.15. EFFECT OF HSM ON HUMAN DERMAL FIBROBLAST .....	17
2.16. EXPRESSION ANALYSIS OF C-MYC IN HEMATOPOIETIC POPULATIONS .....	17
2.17. <i>IN VITRO</i> TREATMENTS .....	17
2.18. <i>IN VIVO</i> TREATMENTS .....	18
2.19. RNA ISOLATION AND CDNA SYNTHESIS .....	18
2.20. REAL-TIME PCR CONFIRMATIONS.....	19
2.21. STATISTICAL ANALYSIS.....	21
3. RESULTS.....	22
3.1. <i>IN VITRO</i> C-MYC INHIBITION INDUCES MOUSE AND HUMAN HEMATOPOIETIC STEM AND PROGENITOR CELL EXPANSION.....	22
3.2. EFFECT OF <i>IN VIVO</i> C-MYC INHIBITION ON HEMATOPOIETIC STEM CELLS .....	27
3.3. C-MYC INHIBITION INHIBITS BM-MSCS PROLIFERATION BUT DO NOT CHANGE PROLIFERATION KINETICS OF AD-MSCS, HUVECS OR HDFS .....	29
3.4. ANALYSIS OF C-MYC TARGET GENE EXPRESSION PROFILE POST TREATMENT WITH 10074-G5.....	30
3.5. INHIBITION OF C-MYC ALLOWS DEVELOPMENT OF <i>EX VIVO</i> HSC EXPANSION COCKTAIL.....	34
4. DISCUSSION.....	35
5. CONCLUSION .....	39
6. FUTURE PROSPECTS.....	41
REFERENCES .....	42
APPENDIX A.....	52

## LIST OF FIGURES

Figure 1.1. The fates of hematopoietic stem cells.....	2
Figure 3.1. Effect of C-myc inhibition on murine HSCs.....	23
Figure 3.2. Effect of c-myc inhibition on human HSPCs.....	24
Figure 3.3. Cell cycle analysis of murine LSK cells after HSM treatments.....	25
Figure 3.4. Apoptosis analysis of murine LSK cells after HSM treatments.....	25
Figure 3.5. Colony-formation assay for lineage negative cells .....	26
Figure 3.6. <i>In vivo</i> c-myc inhibition increased frequency of HSC compartments on murine bone marrow cells.....	28
Figure 3.7. <i>In vivo</i> c-myc inhibition increased mobilization of HSCs to peripheral blood .	28
Figure 3.8. Effect of 10074-G5 on BM-MSC and AD-MSC proliferation .....	29
Figure 3.9. C-myc inhibition do not affect proliferation of human endothelial cell or dermal fibroblast proliferation .....	30
Figure 3.10. The expression analysis of C-Myc in whole bone marrow, lineage negative cells and hematopoietic stem cells.....	31
Figure 3.11. <i>In vitro</i> treatment of lineage negative cells with 10074-G5 downregulates transcription of C-myc .....	31

Figure 3.12. *In vitro* treatment of lineage negative cells with 10074-G5 downregulates transcription of CDKIs and C-myc targets .....32

Figure 3.13. *In vivo* injection of 10074-G5 downregulates the transcription of genes that are downstream of c-myc.....33

Figure 3.14. Combining C-myc inhibitor, 10074-G5, with other HSMs allows robust *ex vivo* expansion of HSPCs.....34



## LIST OF TABLES

Table 1.1. Myc regulates variety of cellular function through its target genes .....	7
Table 1.2. Hematopoietic stem cell phenotype following hematopoietic stem cell specific knockout of genes <i>in vivo</i> .....	9
Table 2.1. Mix of hematopoietic small molecules.....	15
Table 2.2. cDNA reaction mix.....	19
Table 2.3. cDNA reaction conditions .....	19
Table 2.4. List of mouse primers used for Real-time PCR.....	20
Table 2.5. Protocol for qPCR.....	21

## LIST OF SYMBOLS/ABBREVIATIONS

AD-MSC	Adipose derived mesenchymal stem cell
ALL	Acute lymphoblastic leukemia
AML	Acute myeloid leukemia
BM	Bone marrow
BM-MSC	Bone marrow derived mesenchymal stem cells
CDKI	Cyclin dependent kinase inhibitor
CDNA	Complementary deoxyribonucleic acid
CFU	Colony forming unit
CLP	Common lymphoid progenitor
CMP	Common myeloid progenitor
DPBS	Dulbecco's phosphate buffered saline
DMEM	Dulbecco's Modified Eagle Medium
DMSO	Dimethyl sulfoxide
DNA	Deoxyribonucleic acid
ENO1	Enolase 1
ER	Endoplasmic reticulum
ESC	Embryonic stem cells
FACS	Fluorescence-activated cell sorting
FBS	Fetal Bovine Serum
GLUT1	Glucose transporter
HDF	Human dermal fibroblast
HUVEC	Human umbilical cord endothelial cells
HIF-1	Hypoxia Inducible Factor-1
HK2	Hexokinase 2
HPSCs	Hematopoietic progenitor/stem cells
HSCs	Hematopoietic stem cells
HSM	Hematopoietic small molecule
LDHA	Lactate dehydrogenase A
LIN-	Lineage negative cells
L-NIL	L-N 6 -(1-iminoethyl)-lysine hydrochloride

LSK	Lin <sup>-</sup> Sca1 <sup>+</sup> Ckit <sup>+</sup>
LT-HSCs	Long-term hematopoietic stem cells
MEP	Mega-karyotic/erythroid progenitors
MPP	Multipotent progenitors
MSCs	Mesenchymal stem cells
MYC	Myelocytomatosis
NK	Natural killer
NOS	Nitric oxide synthase
PFKM	Phosphofructokinase
PSA	Penicilin Streptomycin Amphicilin
RNA	Ribonucleic acid
RT	Room temperature
SCF	Stem cell factor
SFEM	Serum-Free Expansion Medium
ST-HSC	Short-term hematopoietic stem cells
TUDCA	Tauroursodeoxycholic acid
UCB	Umbilical cord blood
WBM	Whole bone marrow

# 1. INTRODUCTION

## 1.1. HEMATOPOIETIC STEM CELLS

Stem cells are defined as having the capacity to undergo self-renewal and the ability to produce differentiated cells that are required for the tissue homeostasis or repair [1]. One of the important characteristic of stem cells is their potency as they are classified into two groups. Pluripotent embryonic stem cells (ESCs) emerged from inner cell mass of blastocysts and they can differentiate into all types of cells. Adult stem cells, which reside in differentiated tissues considered as multipotent as they can only differentiate into lineage-restricted cells [2]. The hematopoietic stem cells (HSCs) are among the most widely studied and the best-characterized somatic stem cells in the adult. It has been of huge interest for many decades regarding to incredible potential. Two stem cell populations are housed within adult bone marrow: HSCs and mesenchymal stem cells (MSCs) [3]. HSCs are defined by their inherent capacity to self-renew that relies on the ability of a small number of HSCs and to differentiate into all blood cell types [4]. HSCs are classified by their repopulation capacity: the short-term hematopoietic stem cells (ST-HSCs) and long-term hematopoietic stem cells (LT-HSCs). LT-HSCs contain self-renewal capacity during the life of the host species and maintain hematopoietic system. ST-HSCs can only repopulate for about 8 weeks [1]. Following, ST-HSCs form multipotent progenitors (MPP) and then two other types of cells: common lymphoid progenitor (CLPs) and common myeloid progenitors (CMPs). CLPs restricted to give rise to B lymphocytes, T lymphocytes, and natural killer (NK) cells while CMPs only form myelomonocytic progenitors (GMPs) and mega-karyotic/erythroid progenitors (MEPs) (Figure 1.1.) [5].

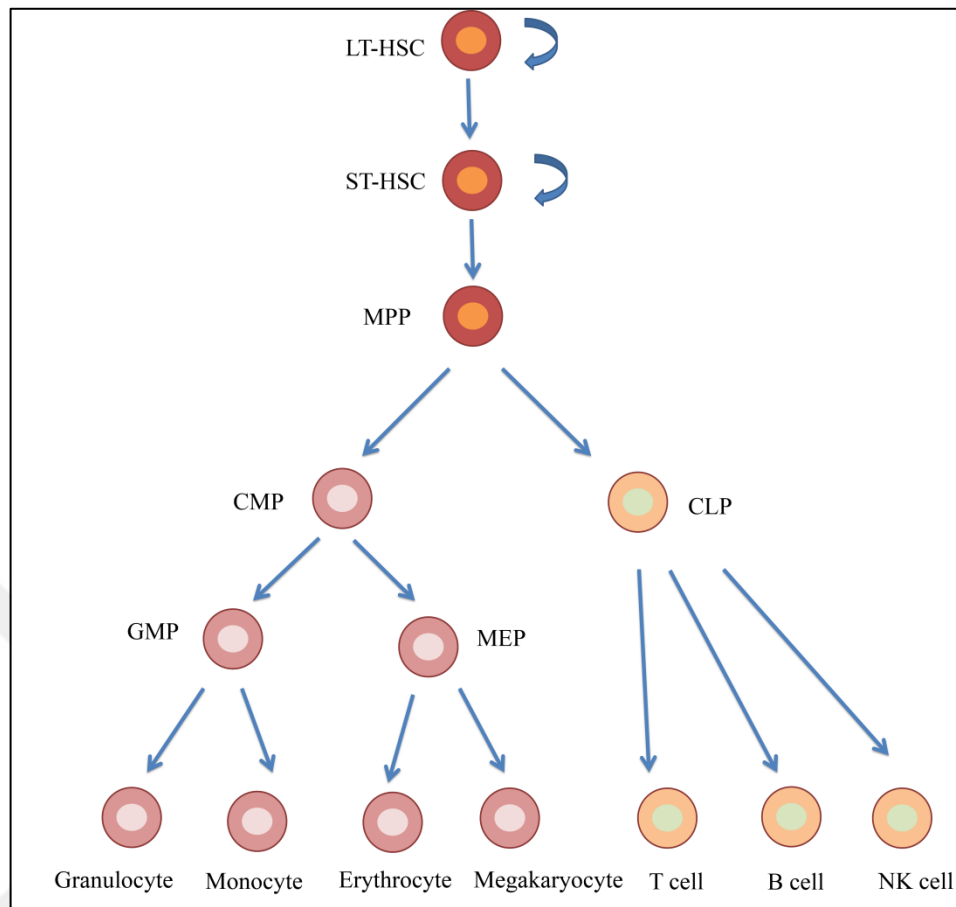


Figure 1.1. The fates of hematopoietic stem cells. Long-Term HSCs (LT-HSCs) are referred as true stem cells of the hematopoietic system and have unlimited self-renewal potential. LT-HSCs produce short-term HSCs (ST-HSCs), which are followed by multipotent progenitors (MPPs) and their differentiation into two major progenitor cell lineages, common myeloid progenitors (CMPs) and common lymphoid progenitors (CLPs). Afterwards they mature into different blood cells.

An emerging hallmark of stem cell is their maintenance in specialized microenvironments, termed a “niche”. HSCs generally reside in endosteal regions of bone marrow (BM) with unique vasculature and restricted perfusion of oxygen, which leads to very low oxygen tension referred as hypoxic niche [6-9]. Stem cells generally reside in quiescent state because of their metabolic adaptation to hypoxic niche [10]. Even though importance of hypoxic conditions was known for several stem cells, there was not enough knowledge about metabolic phenotype and its regulatory pathways or how metabolism relates to the cell cycle of stem cells [11, 12]. To this end, Kocabas and colleagues showed that HSCs in the BM preferably use anaerobic glycolysis rather than mitochondrial oxidative

phosphorylation in order to generate energy [9, 13, 4, 14]. This metabolic phenotype is associated with upregulated expression of hypoxia-inducible factor-1 $\alpha$  (Hif-1 $\alpha$ ) and its downstream target genes, which results in induction of glycolysis and mitochondrial respiration inhibition [4].

## 1.2. *EX VIVO* HSC EXPANSION

HSCs are generally stay in quiescent state and maintained at G<sub>0</sub> phase of the cell cycle and divide only after a stimulus to repopulate all blood cell lineages. Their maintenance during the lifetime of an organism is regulated by complex interplay between cell-intrinsic and cell-extrinsic factors to ensure blood homeostasis [9]. The primarily therapeutic modality for many hematopoietic disorders such as leukemia, lymphoma, some solid cancers and autoimmune disorders is bone marrow transplantation which relies on the ability of a small number of HSCs. However lack of HLA-matched donors limits allogeneic HSC transplantation. Even if a donor is available, higher number of HSCs is needed to reduce toxicity of the procedure and for successful engraftment [15]. This issue has been addressed by developing *ex vivo* methods to expand HSCs. *Ex vivo* HSC expansion approaches mainly rely on growth factors and cytokines [16]. The balance between quiescence and proliferation of HSCs is strictly controlled to maintain homeostasis and ensure HSCs lifelong [17]. However, small molecules that target quiescence factors involved in HSC quiescence have not been widely used for expansion of HSCs. We anticipate that hematopoietic small molecules will bring new approaches to the expansion of HSCs in cell-culture.

*Ex vivo* expansion of HSCs may harbor many difficulties, such as decreased self-renewal ability, senescence, apoptosis, and differentiation. Apart from this, knowledge about constituents of HSC microenvironment and regulators of HSC function in *ex vivo* expansion procedure is restricted. Many studies concentrated on cytokines and growth factors when defining how to expand HSCs in *ex vivo* culture. Cytokines including thrombopoietin (TPO), FL3, IL3, IL6, IL11 and stem cell factor (SCF) have been proved to have function in HSC expansion [16]. Cytokines stimulate HSCs that are arrested in G<sub>0</sub> phase to enter the cell cycle by up-regulating factors responsible in self-renewal and by down-regulating inhibitors of cell cycle. Interestingly, p38 and some other factors that

inhibit cell cycle are upregulated during *ex vivo* expansion procedure [18-20]. Use of p38 inhibitor was shown to increase *ex vivo* expansion of mouse HSCs [18-20]. Earlier studies showed the applicability of *ex vivo* HSC expansion using small molecules [21, 22, 13]. These studies demonstrated the expansion of human and mouse HSCs utilizing Garcinol (non-specific HAT inhibitor), StemRegenin (AhR antagonist) and Nicotinamide (SIRT1 inhibitor) [23, 17, 21, 24]. These studies focused on targeting of cell cycle inhibitors, HSC quiescence regulators and inhibitory factors of *ex vivo* HSC expansion, by applying hematopoietic small molecules (HSMs) [23, 25-28]. One of the recently discovered targets for *ex vivo* expansion of HSCs is Meis1. Kocabas and colleagues have previously reported that HSCs could be expanded *in vivo* by specific deletion of Meis1 or Hif-1 $\alpha$  genes. This expansion of HSCs was evident in increase in HSC frequency, reduction of the number of HSCs in quiescent state (G<sub>0</sub> phase of cell cycle), and induction of percentage of HSCs in G1 and S-G2-M phase of cell cycle [13].

### 1.3. C-MYC GENE

The *c-myc* proto-oncogene was observed in human Burkitt's lymphoma, as a cellular homologue to the viral oncogene (*v-Myc*) of the avian *myelocytomatosis* retrovirus [29, 30]. *Myc* gene family comprises B-Myc, C-Myc, L-Myc, N-Myc, S-Myc that are the basic helix-loop-helix leucine zipper transcription factors. Studies on gene targeting in mice have demonstrated that L-Myc is dispensable [31], however embryos lacking C-Myc or N-Myc cause embryonic lethality [32] and C-Myc and N-Myc can substitute each other [33, 34]. *Myc* proteins have been emerged as essential regulator of variety of cellular processes such as proliferation, cell growth, differentiation, angiogenesis, apoptosis and so on [35, 34, 36]. Many studies showed that upregulated or deregulated expression of *c-myc* gene is related with broad range of cancers such as myeloid leukaemias, melanoma, colon, cervical, breast, small-cell lung carcinomas, osteosarcomas, glioblastomas [29, 37-40]. Although the researches focused on the mechanism in which *Myc* induce tumorigenesis, its physiological function still remains controversial in many tissues *in vivo* [35]. *Myc* was also reported as one of four factors along with Sox2, Oct4, Klf4 that induce mouse embryonic or adult fibroblasts to pluripotent stem cells [41, 39].

#### 1.4. C-MYC TARGET GENES

C-myc has different molecular and cellular effects. These effects arise from changes which mediated by c-myc in large gene families drive cellular functions. Expression studies including SAGE, DNA microarray and hybridization revealed thousands of c-myc target genes [42]. Those can be classified into distinct subgroups. The first proposal that Myc controls energy metabolism by directly activating of genes associated with glycolysis, glutamine metabolism and mitochondrial biogenesis [39]. C-Myc gene involved in glycolysis owing to the detection of lactate dehydrogenase A (LDHA), which generate lactate from pyruvate as part of the glycolytic pathway [43, 42]. Several glucose metabolism genes are also directly regulated by c-Myc, including glucose transporter (GLUT1), phosphofructokinase (PFKM), hexokinase 2 (HK2), and enolase 1 (ENO1) [44-47]. Through the upregulation of these downstream targets, c-myc induces the Warburg effect which enables generation of pyruvate from glucose even under adequate oxygen tension. Many cancer cells apply to aerobic glycolysis termed Warburg effect to meet their energy demand in comparison to normal differentiated cells which mainly use mitochondrial oxidative phosphorylation [48]. Besides, p53 tumor suppressor protein was shown to regulate mitochondrial function and glycolysis in which its absence is linked with elevated aerobic glycolysis [49]. The hypoxia inducible factor, Hif-1 $\alpha$ , is an essential regulatory transcription factor for cellular and systemic responses in hypoxic conditions. Hif-1 $\alpha$  induces glycolysis by stimulating the expression of glucose transporters and glycolytic enzymes such as LDHA, HK2, enolase and aldolase [50]. Additionally, it causes a shift from mitochondrial oxidative phosphorylation to glycolysis as a result of inhibition of mitochondrial biogenesis [48]. Myc expression can be repressed by Hif-1 $\alpha$  transcription factor under hypoxic conditions [51, 52] but on the other hand, its deregulated expression cooperates with Hif-1 $\alpha$  to stimulate glycolysis for cancer cell growth [39, 53]. Also it has already been known that Hif-1 $\alpha$  has a key role in maintaining quiescence of HSCs as well [54].

One another important function of c-myc is its ability to induce cell proliferation. Previous studies revealed the role of c-myc in cell cycle regulation [37]. Myc controls cell cycle progress by activating cyclins D1, D2, E1, A2 as well as CDK4. Its function in cell proliferation not only limited with this but also it regulates cell cycle by elimination of cell

cycle checkpoints and inhibition of the cyclin-dependent kinase (CDK) inhibitors (CDKIs) [55]. It has been reported that c-myc inhibits CDKI p15<sup>Ink4a</sup> and p21<sup>Cip1</sup> through interplay with Miz1 protein at the core promoter [56-58]. c-Myc regulates HSC proliferation and long-term self-renewal by repressing p21<sup>Cip1</sup> [59, 60]. While expression of Myc in variety of cell types dramatically blocks the differentiation, it could also stimulate cellular differentiation [55, 61-64]. It has been suggested that downregulation of Myc is necessary for cell exit from the cycle and undergoing differentiation, further this suggestion strengthened by the induction and function of the Mxd family members in response to differentiation cues [55]. In the non-existence of specific survival factors, deregulated Myc expression promotes default pathway of cell death, apoptosis [65, 66, 55]. Deregulated Myc is associated with hyper proliferative state of cells, which is also controlled with increased apoptosis [67]. Once Myc-induced apoptosis was abrogated, it can be resulted in clonal tumors. This pivotal function of Myc in apoptosis was elucidated by the study in Myc-deficient cells, which showed that Myc-deficient cells were capable to resist to variety of apoptotic signals [68, 69]. However, there is no definite molecular mechanism of Myc-induced apoptosis has defined, it seems that multiple pathways has involved in triggering apoptosis. A study showed that deregulated Myc activates the tumour suppressor p53 and induces cell death [70]. Another study reported that Myc triggers apoptosis by stimulating Arf, which in turn activates p53 to regulate downstream targets [71, 55]. Elucidation of the pathways through Myc-induced apoptosis can shed light to self-destruction of Myc deregulated tumours.

Cadherins and integrins have been shown to synergistically control mobility and migration of cells. C-Myc has been shown to play a role in HSCs to exit from the stem cell niche through the down-regulation of N-cadherin. C-Myc deficient HSCs showed increased levels of N-cadherin and this indicated that mutant stem cells are remained in the niche. Additionally, c-myc suppress expression of some of the integrin family members such as VLA-5 and LFA-1 [60, 37].

Table 1.1. Myc regulates variety of cellular function through its target genes.

Function	Regulation	Target genes
Energy metabolism eg. glycolysis, mitochondrial biogenesis	Up	Ldha, Pfkfb3, Glut1, Hk2, Eno1, Hif-1 $\alpha$
Cell cycle	Up	Cyclin D2, Cdk4
Differentiation and resistance to growth arrest	Down	p15 <sup>INK4B</sup> , p21 <sup>CIP1</sup> , CEBP
Apoptosis	Up	p53, p19 <sup>Arf</sup>
Cell adhesion and migration	Down	Integrin, N-cadherin
Transformation	Up	Diverse group of genes are thought to play
Stem cell self-renewal activity	Up	Genes associated with cell cycle, cell death and metabolism

### 1.5. SMALL MOLECULE TARGETED *EX VIVO* HSC EXPANSION

Under steady state, HSCs are maintained quiescent within the stem cell niche in the BM [72]. HSCs' ability to proliferate is restricted in culture compared to their strong capacity *in vivo*. To expand HSCs for clinical use, specific hematopoietic growth factors have been used or cells were induced by specific HSC regulators *in vitro*. The elucidation of specific HSC regulators revealed limited number of genes that play major role in self-renewal of HSCs. Wilson et al. showed that conditional deletion of, an oncogene, C-Myc, in contrast to decrease in lineage positive cells, intriguingly increased lineage negative cells about 3-fold 3 week after post deletion *in vivo*. Ckit<sup>+</sup>Lin<sup>-</sup>Sca1<sup>+</sup> (KLS) subpopulation was enriched more than 20-fold in C-Myc deficient bone marrow compared with control bone marrow. This corresponds to about 3-fold enrichment in the absolute number of Lin<sup>-</sup>Sca1<sup>+</sup>Ckit<sup>+</sup> cells (Table 1.2) [60]. To date, there is no shown any therapeutic agent that targets c-myc for expanding HSCs *ex vivo*. We have found that 10074-G5 is a promising c-myc inhibitor that

targets myc/max interaction. By using 10074-G5, it will be possible to safely expand HSCs.

Small molecules that are natural and chemically synthesized products have important role in molecular biology and in clinical therapy via pharmaceuticals. Small molecules has also assisted the exploration of the signaling pathways which regulate stemness and been used to expand HSCs *ex vivo* [23]. The function of  $\alpha$ -tocopherol, tauroursodeoxycholic acid (TUDCA) and L-N-6-(1-iminoethyl)-lysine hydrochloride (L-NIL) on hematopoietic stem has been shown previously.  $\alpha$ -Tocopherol is a member of the vitamin E family which has many biological features. Tocopherols have been shown that they could induce or inhibit growth of variety of cell types. It has been thought that tocopherols play role in the expansion of primitive hematopoietic cells through its radioprotective property [73]. According to the immunohistochemistry and flow cytometry analysis, frequency of BrdU within whole BM cells and within the c-Kit population increased, besides HSC/HP cells which are in S/G2/M phase increased after  $\alpha$ -tocopherol treatment [73]. Dppa5 is a regulator of survival and functional HSC activation by diminishing endoplasmic reticulum (ER) stress. Dppa5 overexpression showed robust increase in the reconstitution capacity of HSCs and ER stress after *in vitro* culture. For this reason, it is suggested that reducing ER stress levels by using chemical chaperones, like TUDCA, is a potential treatment for promoting HSC reconstitution capacity by providing clue that ER stress reduction *in vitro* resulted in robust increase in engraftment of functional HSCs [72, 74]. CD34<sup>+</sup>48<sup>-</sup>KSL cells were cultured with TUDCA for 14 days and they found that TUDCA treatment increased total hematopoietic cell number and the percentage of CD34<sup>+</sup>48<sup>-</sup> KSL cells [72]. iNOS (nitric oxide synthase) has been detected in hematopoietic cells and many other cell types [74]. It has been reported that highly purified human CD34<sup>+</sup> progenitor cells contain iNOS and NO was found to show inhibitory role on human hematopoiesis [75]. Treatment with the selective iNOS inhibitor, L-NIL, increased preservation of CD34<sup>+</sup> progenitors by highlighting that it could be useful for *ex vivo* expansion of progenitor cells [74].

Table 1.2. Hematopoietic stem cell phenotype following hematopoietic stem cell specific knockout of genes *in vivo*.

<b>Small Molecule</b>	<b>Target Gene</b>	<b>Average Fold Increase in % of HSCs</b>	<b>References</b>
10074-G5	C-Myc	4.0	Wilson et al.,2004
TUDCA	Unidentified	3.1	Miharada et al., 2014
$\alpha$ -Tocopherol	Unidentified	1.7	Nogueira et al., 2011
L-NIL	i-NOS	1.3	Reykdal et al., 1999

The use of hematopoietic small molecules (HSMs) become instrumental in developing new approach to expand and maintain functional HSCs *ex vivo* and may have a potential for improving clinical transplantation of HSCs in the future. In this study, novel c-myc inhibitor 10074-G5, TUDCA,  $\alpha$ -tocopherol and L-NIL have been utilized to expand HSCs *ex vivo*. C-myc inhibitor, 10074-G5, might represent a promising novel inhibitor for HSPC/HSC expansion alone or in combination with other small molecules that we tested.

## **2. MATERIALS AND METHODS**

### **2.1. MATERIALS AND ANIMAL INFORMATION**

Cells were treated with the most effective dose of 10074-G5 (Calbiochem, Cat no.475957), TUDCA (Calbiochem, Cat no.580549-16M),  $\alpha$ -Tocopherol (Sigma Aldrich, Cat no. 258024-5G) and L-NIL (Enzo, Cat no.ALX-270-010-M010) at a concentration of 10  $\mu$ M, dissolved in Dimethyl sulfoxide. Dimethyl sulfoxide (% 0.5) used as a control (DMSO, Santa Cruz Biotech, cat. no. sc-3590329). All human and animal studies were approved by the Institutional Clinical Studies Ethical Committee of Yeditepe University (Decision numbers 547 and 548), and the Institutional Animal Care and Use Committee of Yeditepe University (YUDHEK, decision number 429). Balb/c mice have been used in the studies.

### **2.2. BONE MARROW COLLECTION AND MAGNETIC LINEAGE DEPLETION**

Bone marrow cells were harvested from femur and tibia of 6-8 week Balb/c mice (YUDETAM, Turkey) following euthanasia. After animal skeletons were rinsed with 70% ethanol, dissections were performed under the hood. A skin incision was performed around the perimeter of hind limbs, and then the skin pulled toward the foot which is cut at the ankle bone. Hind limbs were dissected and stored in ice cold Dulbecco's phosphate-buffered saline (DPBS, Invitrogen, Gibco, UK, cat. no.14190250). The hind limbs were cut off through the knee joint. Femur and tibia were cleaned from muscle and connective tissues by scraping with scalpels. Bone marrow cells were harvested by flushing femurs and tibias with ice cold DPBS using a syringe and a 26G needle. The cell suspension was filtered through 70- $\mu$ m cell strainer (BD Pharmingen, cat. no. 352350). The yield of cells were assessed by counting on a hemocytometer and then centrifuged at 1500 rpm for 5 minutes. After this step, magnetic cell separation was performed according to a protocol modified from mouse hematopoietic progenitor (stem) cell enrichment set - DM (BD Pharmingen, cat. no. 558451). The supernatant was removed and for each  $50 \times 10^6$  cells the following quantity of materials were used. Cells were resuspended in 0,5 ml ice cold DPBS

supplemented with 2% (v/v) fetal bovine serum (FBS, Sigma Aldrich, USA, cat. no. 12103C) and then 5µl BD Fc Block™ was added and incubated on ice for 15 minutes. 25 µl Biotinylated Mouse Lineage Depletion Cocktail was added to cell suspension incubated on ice for 15 minutes then washed with 10 ml DPBS supplemented with 2% (v/v) FBS and spinned at 1500 rpm for 5 minutes. After removing of supernatant, cells were resuspended in 225 µl DPBS supplemented with 2% (v/v) FBS. Then cells were labeled with 25µl BD IMag™ Streptavidin Particles Plus on ice for up to 30-minute incubation. Cell suspension were washed with 10 ml DPBS supplemented with 2% (v/v) FBS, spinned at 1500 rpm for 15 minutes and supernatant was removed respectively. Labeled cell suspension is then placed within the magnetic field of the IMagnet (BD Pharmingen cat. no. 552311) by dissolving in 3 ml DPBS supplemented with 2% (v/v) FBS. Labelled cells were transferred to a 12x75 mm round bottom test tube and placed on IMagnet for 10 minutes. After 10 minutes, the supernatant (negative fraction) was aspirated without disturbing the tube and placed in a 2<sup>nd</sup> new sterile tube for 10 minutes. The positive fraction was resuspended in same volume DPBS supplemented with 2% (v/v) FBS and placed on IMagnet for another 10 minutes. Supernatant was aspirated from 2<sup>nd</sup> tube and transferred to 15 ml falcon tube after 10 minutes. Supernatant from 1<sup>st</sup> tube was transferred to new tube and placed on IMagnet for 10 minutes. End of time, supernatant was added to cell suspension in 15 ml falcon tube. The final depleted fraction contains lineage negative cells.

### **2.3. HEMATOPOIETIC STEM CELL STAINING OF MURINE BONE MARROW CELLS AND FLOW CYTOMETRY ANALYSIS**

Lineage negative cells (30,000 cells/well) were cultured on a 96 well plate (Corning Costar, cat no. CLS3599) in Serum-Free Expansion Medium (StemSpan SFEM, Stemcell technologies, cat no. 09650) supplemented with SCF (1000 unit/mL), TPO (1000 unit/mL), FLT-3L (5000 unit/mL) (all from R&D Systems Inc., Minneapolis) and 1% (v/v) PSA (10,000 units/ml penicillin and 10,000 ug/ml streptomycin and 25 µg/mL of Amphotericin B, Gibco, cat.no.15240062) and treated with small molecules for 7 days. Cells were stained with HSC markers according to the manufacturer's protocol. Following antibodies were used for identification of LSK and LSKCD34<sup>low</sup> populations: Anti-Mouse CD16/32 Fc block, c-Kit (CD117) PE, CD34 FITC, Sca-1 PE-Cy7 and mouse APC lineage cocktail (BD StemFlow, cat no. 560492). Two separate mix was prepared with antibodies given

above. As a first step 50  $\mu$ l mix 1 (5 ml DPBS and 2  $\mu$ l Fc block) was added to the cells and mixed by pipetting 3-4 times then incubated for 10 minutes at room temperature. 50  $\mu$ l mix 2 (5 ml DPBS and 2ul lineage cocktail, 2ul Sca-1, 2ul c-kit, 2ul CD34 FITC antibodies) was added and mixed by pipetting 3-4 times then incubated for 15 minutes at room temperature. Cell kinetics was analyzed by flow cytometry analysis (FACSARIA III, BD, cat. no. 23-11539-00).

#### **2.4. CELL COUNTING AND IMAGING**

Lineage negative cells were seeded at a density of 30.000 cells/well on a 96-well plate in SFEM media supplemented with SCF (1000 unit/mL), TPO (1000 unit/mL), FLT-3L (5000 unit/mL) and 1% (v/v) PSA. Cells were treated with small molecules and DMSO (%0,5) used as a control. After 4 days treatment, cells were stained with Hoechst 33342 (10 $\mu$ g/ml) (Sigma Aldrich, USA, cat no. 14533). Cells were screened under fluorescent microscope at day 4, 7 and 10 and images were taken respectively. Cell count was assessed using Scion image program.

#### **2.5. UMBILICAL CORD BLOOD CELL ISOLATION**

UCB mononuclear cells were isolated by Ficoll-Paque (Histopaque<sup>TM</sup>, Sigma, cat. no.10831) density gradient centrifugation. 15 ml cord blood was diluted with DPBS as 1:1 proportion in a 50 ml falcon tube and mixed gently by inverting. Cord blood was underlaid with 15 ml Ficoll-Paque and centrifuged at 3000 rpm for 15 minutes without brake. After centrifugation upper phase was removed and cloudy interphase transferred to new 50 ml falcon tube. Mononuclear cells were washed with 3x volume DPBS and mixed by gentle inverting. Cells were centrifuged at 1500 rpm for 5 minutes with brake, and then supernatant was removed. Cell pellet was suspended in 10 ml DPBS and cell density was assessed by counting on hemocytometer. UCB mononuclear cells were seeded on 96 well-plate in expansion medium at 10,000 cells per well for flow cytometry analysis. The expansion medium consists of Serum-Free Expansion Medium (StemSpan<sup>TM</sup> Serum-Free Expansion Medium (SFEM), Stemcell Technologies, cat. no. 09650) supplemented with human cytokine cocktail (StemSpan<sup>TM</sup> CC100, Stemcell Technologies, cat. no. 02690) and

1% PSA (10,000 units/ml penicillin and 10,000 ug/ml streptomycin and 25 µg/mL of Amphotericin B, Gibco, cat. no.15240062). The seeded cells were treated with three different concentrations of HSMs as final concentrations of 0.1 µm, 1µm and 10µm. DMSO (%0.5) treated cells were used as a control.

## **2.6. FLOW CYTOMETRY ANALYSIS OF HUMAN HSPCS**

After 7 days of the treatment with the small molecules, the UCB mononuclear cells were labelled with PE-conjugated anti-human CD34 (Biolegend, Cat.No.343506), APC-conjugated anti-human CD133 (Miltenyibiotec, Order No.130-090-826) antibodies and treated with Aldefluor reagent (ALDEFLUOR™ Kit, Stemcell Technologies, Cat.No. 01700) according to the manufacturer's manual (Stemcell Technologies). The expressions of CD34 and CD133 surface markers and ALDH (Aldehyde Dehydrogenase) enzyme activity in the labelled cells were analyzed by flow cytometry (FACSARIA III, BD, cat. no. 23-11539-00).

## **2.7. CELL CYCLE ANALYSIS OF MURINE LSK CELLS**

To perform cell cycle analysis, murine LSK (Lin<sup>-</sup>Sca1<sup>+</sup>C-kit<sup>+</sup>) cells from mouse lineage negative cell population were sorted by flow cytometry (FACSARIA III, BD Biosciences, cat. no. 23-11539-00). Lineage negative cells were suspended in 500 µl DPBS supplemented with 2% FBS and were stained with each 2 µl mouse APC lineage cocktail, anti-Mouse c-Kit (CD117) PE, Sca-1 PE-Cy7. Cells were stained with antibodies on ice for 15 minutes. Murine LSK cells were seeded on the proper expansion medium at a density of 5,000 cells per well in 96 well-plate. They were treated with the effective doses of 10074-G5, TUDCA, α-Tocopherol, and L-NIL at 10 µm concentration. After 3 days of the treatment, the cells were stained with 2 µl of 100X Hoechst 33342 (10 µg/ml) (Sigma Aldrich, USA, cat no. 14533) and incubated in humidified incubator at 37°C and 5% CO<sub>2</sub> for 30 minutes. Then, 1 µl of Pyronin Y (100 µg/ml) (Sigma Aldrich, USA, cat no. P9172-1G) was added and incubated for 15 minutes in humidified incubator at 37°C and 5% CO<sub>2</sub>. Stained cells were transferred to sterile flow tubes and cell cycle kinetics was analyzed by flow cytometry.

## **2.8. APOPTOSIS ANALYSIS OF MURINE LSK CELLS**

Murine Lin<sup>-</sup>Sca1<sup>+</sup>Kit<sup>+</sup> (LSK) cells were isolated by flow cytometry from lineage negative cells (FACS Aria III, BD Pharmingen, cat no. 23- 11539-00). Murine LSK cells were seeded at a density of 5000 cells/well in 96-well plates and treated with HSMs in three replicates at a final concentration of 10 μM for 3 days in the humidified incubator at 37°C and 5% CO<sub>2</sub>. 3 days after, cells were collected from 96-well plates and centrifuged at 1500 rpm for 5 minutes. After removing of supernatant, cells were suspended in 50 μl 1X binding buffer (BD Pharmingen, cat no 556570) and then stained according to the manufacturer's manual (BD Pharmingen, cat no 556570) with 1 μl FITC Annexin V and 1 μl PI at room temperature for 15 minutes. After incubation time, 200 μl 1X binding buffer were added onto cells and mixed by pipetting. Samples were analyzed by flow cytometry (FACS Aria III, BD Biosciences, cat no. 23- 11539-00).

## **2.9. COLONY FORMATION UNIT (CFU) ASSAY**

To perform colony-forming unit assay, the depleted murine lineage (-) cells (30,000 cells/well) were treated with the most effective doses of 10074-G5, TUDCA, α-Tocopherol, and L-NIL at 10 μM concentration. After 7-day expansion, the cells were harvested and counted. Then the cells were plated in methylcellulose-containing medium (MethoCult™ GF M3434, Stemcell Technologies, Cat.No. 03444) at a density of 65,000 cells per well in 6-well plate, performed in triplicate. After 10-14 days, colonies were classified as CFU-GEMM, CFU-G/M, BFU-E colonies and counted by inverted microscope.

## **2.10. COMBINATORIAL HSM TREATMENTS**

Small molecule cocktails prepared as it contains all combinations of these four small molecules. Each small molecule concentration is 1mM within its cocktail. 30,000 lineage negative cells per well were treated with small molecule mixes in 96-well plates at a final concentration of 10 μM during 7 days for flow cytometry analysis.

Table 2.1. Mix of hematopoietic small molecules.

	M5	M6	M7	M8	M9	M10	M11	M12	M13	M14	M15
<b>10074-G5</b>	+	+	+	-	-	-	+	+	+	-	+
<b>TUDCA</b>	+	-	-	+	+	-	+	+	-	+	+
<b><math>\alpha</math>-Tocopherol</b>	-	+	-	+	-	+	+	-	+	+	+
<b>L-NIL</b>	-	-	+	-	+	+	-	+	+	+	+

### 2.11. BONE MARROW-DERIVED MESENCHYMAL STEM CELL ISOLATION

Mouse bone marrow mesenchymal stem cells were isolated according to a protocol modified from Soleimani and Nadri [3]. Bone marrow cells were collected as described above and seeded at a density of  $30 \times 10^6$  cells in T-75cm<sup>2</sup> flasks (Sigma Aldrich, cat no. CLS3290) in Dulbecco's Modified Eagle's Medium (DMEM, Gibco) supplemented with 15% (v/v) FBS (Sigma Aldrich, USA, cat no. 12103C) and 1% (v/v) PSA (10,000 units/ml penicillin and 10,000 ug/ml streptomycin and 25  $\mu$ g/mL of amphotericin B, Gibco, Cat.No.15240062). One day after, non-adherent cells were removed and medium was changed in every 3-4 days. After 15 days of initiating culture, MSCs were lifted with 0.25% tyripsin-EDTA (Sigma Aldrich, USA, cat no. 25200056) and cultured in T75 cm<sup>2</sup> flasks. 10,000 BM-MSCs per well were seeded on a 96-well plate for small molecule treatments. The seeded cells were treated with three different concentrations of HSMs as final concentrations of 0,1  $\mu$ m, 1  $\mu$ m and 10  $\mu$ m.

### 2.12. ADIPOSE-DERIVED MESENCHYMAL STEM CELL ISOLATION

Adipose tissue was collected from liposuction operation and MSC isolation was performed within 1 hour. 60 ml adipose tissue was placed into a 500 ml bottle and same amount of collagenase solution was added. The tissue was digested at 37°C for 1 hour by continuous shaking. The digested tissue was centrifuged at 2500 rpm for 7 min at room temperature (RT). The adult adipocytes and collagenase solution the supernatant discarded and the

pellet was resuspended with 2 ml of erythrocyte lysis buffer. The cell suspension was completed to 50 ml with erythrocyte lysis buffer and incubated at 37°C for 10 min by continuous shaking. The cell suspension was centrifuged at 1400 rpm for 7 min at RT and supernatant was discarded. The pelleted cells were washed with 1X PBS then centrifuged at 1400 rpm for 7 min at RT, supernatant were discarded. The cells were resuspended in 6-8 ml DMEM (Gibco) then filtered through 100 µm cell strainer. The cells seeded onto tissue culture polystyrene flasks as  $10^6$  cells/150 cm<sup>2</sup>. After 24 hour cultured, the cells washed with 1X DPBS and the medium is refreshed.

10,000 AD-MSCs per well were seeded on a 96 well plate for small molecule treatment. The seeded cells were treated with three different concentrations of HSMs as final concentrations of 0,1 µm, 1 µm and 10 µm.

### **2.13. WST1 ANALYSIS**

Mouse BM-MSCs and human AD-MSCs were seeded in 96 well plates at a density of 5,000 cell and 10,000 cell per well respectively. Cells were treated with three different concentrations of HSMs as final concentrations of 0,1 µm, 1 µm and 10 µm for three days. Three days after, cell medium was removed. WST1 reagent were diluted in 1:10 range with culture medium (Cell Proliferation Reagent WST-1, Roche, cat. no. 11644807001) and added as 50 µl for each sample and one blank sample. Plates were incubated in humidified incubator at 37°C and 5% CO<sub>2</sub> in dark and measured the absorbance of the samples at the time point of 1 hour, 2 hours and 3 hours using a microplate reader at 420-480 nm.

### **2.14. EFFECT OF HSM ON HUVEC**

Human umbilical cord endothelial cells (HUVECs, ATCC® CRL1730™) were seeded on 96 well plates at a density of 2,000 cells per well. One day after, small molecules were added into each well with 0.1, 1 and 10 µM concentrations. Cell viability in each well has been measured by using WST1 cell proliferation reagent (Cell Proliferation Reagent WST-1, Roche, cat. no. 11644807001) 3 days after treatment.

## **2.15. EFFECT OF HSM ON HUMAN DERMAL FIBROBLAST**

Human dermal fibroblast (HDF) cells were kindly provided by Dilek Telci from Yeditepe University, Turkey. Cells were dissolved in the room temperature (RT) and 3-4  $\mu$ l DMEM supplemented with 10% (v/v) FBS (Sigma Aldrich, USA, cat. no. 12103C) and 1% (v/v) PSA (10.000 units/mL penicillin, 10.000  $\mu$ g/mL streptomycin, 25  $\mu$ g/mL amphotericin B) (Invitrogen, Gibco, UK) were added into the cell suspension. The cells were centrifuged at 300 x g for 5 minutes at RT and the pellet was resuspended in fresh medium and transferred into a T-75cm<sup>2</sup> flask (Sigma Aldrich, USA, cat. no. CLS3289). The cells were incubated in the humidified incubator at 37°C and 5% CO<sub>2</sub>. HDF cells were seeded at a density of 5000 cells per well in 96-well plates and treated with 0,1, 1 and 10  $\mu$ M concentrations for cell viability WST1 assay.

## **2.16. EXPRESSION ANALYSIS OF C-MYC IN HEMATOPOIETIC POPULATIONS**

Whole bone marrow was harvested from Balb/c mouse and lineage negative cells were isolated as described before. Lin<sup>-</sup> cells were stained with following stem cell markers in order to isolate HSCs (Lin-Sca1+Ckit+CD34<sup>-</sup>). 325,000 LSKCD34<sup>-</sup> cells were isolated by FACS Aria III, (BD Biosciences, cat no. 23- 11539-00). Supernatant was removed and pellet was stored at -80°C. Additionally, 2x10<sup>6</sup> cells from WBM and 3x10<sup>6</sup> Lin<sup>-</sup> cells were separated for further RNA isolation and confirmation of C-Myc expression by Real-time PCR.

## **2.17. IN VITRO TREATMENTS**

Lineage negative cells were isolated from Balb/c mouse as described. 2x10<sup>6</sup> lin<sup>-</sup> cells were seeded on a 6-well plate and treated with DMSO control (%0.5) and 10 $\mu$ M dose of 10074-G5 for 5 days in 37°C humidified incubator. After treatment, cells were collected for RNA isolation in 15ml falcon tubes at -80°C.

## 2.18. *IN VIVO* TREATMENTS

10074-G5 was diluted in 100  $\mu$ l PBS at a concentration of 1 $\mu$ M for *in vivo* studies. In this aim, 100  $\mu$ l 10074-G5 was injected into adult wild type Balb/c mice intraperitoneally on 1<sup>st</sup>, 5<sup>th</sup> and 7<sup>th</sup> days as three doses. Following three doses of treatment, at 10<sup>th</sup>, day mice were euthanized. Bone marrow cells were harvested from femur and tibia and analyzed by flow cytometry following staining with APC lineage cocktail, c-Kit (CD117) PE, Sca-1 PE-Cy7, CD150 FITC and CD48 APC. Moreover, to measure HSC mobilization peripheral blood was collected through retroorbital bleeding and stained with APC lineage cocktail, c-Kit (CD117) PE, Sca-1 PE-Cy7, CD34 FITC then analyzed by flow cytometry.

## 2.19. RNA ISOLATION AND CDNA SYNTHESIS

RNA was isolated according to the manufacturer's protocol GenElute™ Mammalian Total RNA Miniprep Kit (Sigma Aldrich, Cat no. RTN70). Cells were pelleted by centrifuging at 1500 rpm for 5 minutes. Culture medium was removed completely. 250  $\mu$ l lysis solution/2-Mercaptoethanol was added into each tube and vortexed until all clumps disappear. Lysed cells were loaded into GenElute Filtration Columns and then centrifuged at 13,000xg for 2 minutes. Filtration column was discarded, 250  $\mu$ l 70% ethanol was added to the filtered lysate and pipetted to mix. This lysate was transferred to GenElute Binding Column and next centrifuged at 13,000xg for 15 seconds. Flow-through liquid was discarded. 500  $\mu$ l Washing Solution-I was added to the column and centrifuged again at same speed for 15 seconds. After centrifugation, binding column was inserted into new collection tube. The binding column was washed with 500  $\mu$ l Washing Solution-II, centrifuged at same speed for 15 seconds and then flow-through was discarded. This step was repeated two times. Binding column was dried with additional centrifugation and then eluted with 30  $\mu$ l Elution buffer.

RNAs were converted to cDNA by using ProtoScript® First Strand cDNA Synthesis Kit (NEB, Cat no. E6300S). All eluted RNA was used as a template and 0.5-1  $\mu$ g cDNA was synthesized. Each RNA sample was mixed with 2  $\mu$ l random primer and denatured at 65°C for 5 minutes and then transferred into ice. Reaction mix (12  $\mu$ l) and Enzyme mix (2  $\mu$ l) for each RNA sample were mixed in one eppendorf tube and shared (Table 2.2). Reaction

was conducted in BioRad PCR in following conditions for maximum yield and length: 25°C for 5 min, 42°C for 60 min (2X cycle), 80°C for 5 min and 4°C (Table 2.3)

Table 2.2. cDNA reaction mix

RNA sample (0.5-1 µg)	30 µl
Random primer (10X)	2 µl
Reaction mix (3X)	12 µl
Enzyme mix (30X)	2 µl
<b>Total volume</b>	<b>46 µl</b>

Table 2.3. cDNA reaction conditions

<b>Temperature</b>	<b>Time</b>
25°C	5 min
42°C	60 min (2X cycle)
80°C	5 min
4°C	∞

## 2.20. REAL-TIME PCR CONFIRMATIONS

Pre-designed primers (Table 2.4) obtained from NIH Mouse depot (<https://mouseprimerdepot.nci.nih.gov/>) ordered from Sentegen Biotechnology. Maxima SYBR Green qPCR Master Mix (2X) (Thermo Scientific, Cat. No. K0222) was used in order to perform Real-time PCR. Reaction was conducted on BioRad CFX96 Touch™ Real-Time PCR Detection System. Data were analyzed by using  $\Delta\Delta C_t$  method and  $\beta$ -actin was used as a housekeeping gene to normalize results. Quantity of components of reaction were given in Table 2.5.

Table 2.4. List of mouse primers used for Real-time PCR

<b>Gene</b>	<b>Forward Primer</b>	<b>Reverse Primer</b>
$\beta$ -actin	ATGGAGGGGAATACAGCCC	TTCTTTGCAGCTCCTTCGTT
LDHA	CTGGGTCCTGGGAGAACAT	GTGCCCAGTTCTGGGTAAAG
Glut-1	AACACTGGTGTCAACACGC	GAGTGTGGTGGATGGGATG
Eno-1	CACCCTCTTTCCTTGCTTTG	AGATCGACCTCAACAGTGGG
HK-2	GGAGCTCAACCAAACCAAG	GGAACCGCCTAGAAATCTCC
PFKM	CCATGAAGAGCATCATGCAG	AGCATTACATACCTTGGGCAT
Myc	TGAAGTTCACGTTGAGGGG	AGAGCTCCTCGAGCTGTTTG
p15	CAGTTGGGTTCTGCTCCGT	AGATCCCAACGCCCTGAAC
p16	GGGTTTCGCCCAACGCCCCGA	TGCAGCACCACCAGCGTGTC
p18	CTCCGGATTTCCAAGTTTCA	GGGGGACCTAGAGCAACTTAC
p19	TCAGGAGCTCCAAAGCAACT	TTCTTCATCGGGAGCTGGT
p19arf	GTTTTCTTGGTGAAGTTCGTGC	TCATCACCTGGTCCAGGATTC
p21	ATCACCAGGATTGGACATGG	CGGTGTCAGAGTCTAGGGGA
p27	GGGAACCGTCTGAAACATT	AGTGTCCAGGGATGAGGAAG
p57	TTCTCCTGCGCAGTTCTCTT	CTGAAGGACCAGCCTCTCTC
Trp53	CTAGCATTCAGGCCCTCATC	AATGTCTCCTGGCTCAGAGG

Table 2.5. Protocol for qPCR

<b>Component</b>	
Maxima SYBR Green qPCR Master Mix (2X)	7.5 $\mu$ l
Water (nuclease free)	4 $\mu$ l
Forward Primer (10 $\mu$ M stock conc.)	0.75 $\mu$ l
Reverse Primer (10 $\mu$ M stock conc.)	0.75 $\mu$ l
DNA sample	2 $\mu$ l
<b>Total volume</b>	<b>15 <math>\mu</math>l</b>

## 2.21. STATISTICAL ANALYSIS

Results are expressed as mean  $\pm$  SEM and a 2-tailed Student *t* test was used to determine the level of significance.  $p < 0.05$  was considered statistically different.

### 3. RESULTS

#### 3.1. *IN VITRO* C-MYC INHIBITION INDUCES MOUSE AND HUMAN HEMATOPOIETIC STEM AND PROGENITOR CELL EXPANSION

Sufficient number of HSCs is needed for effective transplantation and engraftment. This requires expansion of functional HSCs which is safe to the recipients. We analyzed the frequency of HSCs in DMSO and HSMs treated HSC cultures following 7 days of expansion procedure by flow cytometry after staining with corresponding surface antigens (Lin<sup>-</sup>Sca1<sup>+</sup>Kit<sup>+</sup>CD34<sup>-</sup>). 10074-G5 and tested HSMs decreased C-kit<sup>+</sup> level (Figure 3.1A) however, they increased Sca1<sup>+</sup> expression gradually (Figure 3.1B). C-myc inhibitor 10074-G5 significantly increased LSK (0.95%) and LSKCD34<sup>low</sup> (0.41%) compartment compared to DMSO control (0.54% and 0.25% respectively) (p<0.01) (Figure 3.1C and 3.1D). It led to more than 1.5-fold increase in LSK and LSKCD34<sup>low</sup> compartment (Figure A.2). Additionally, TUDCA,  $\alpha$ -Tocopherol and L-NIL was responsible of increased frequencies of LSKCD34<sup>low</sup> compartment (0.55%, 1.17% and 0.5%, respectively).

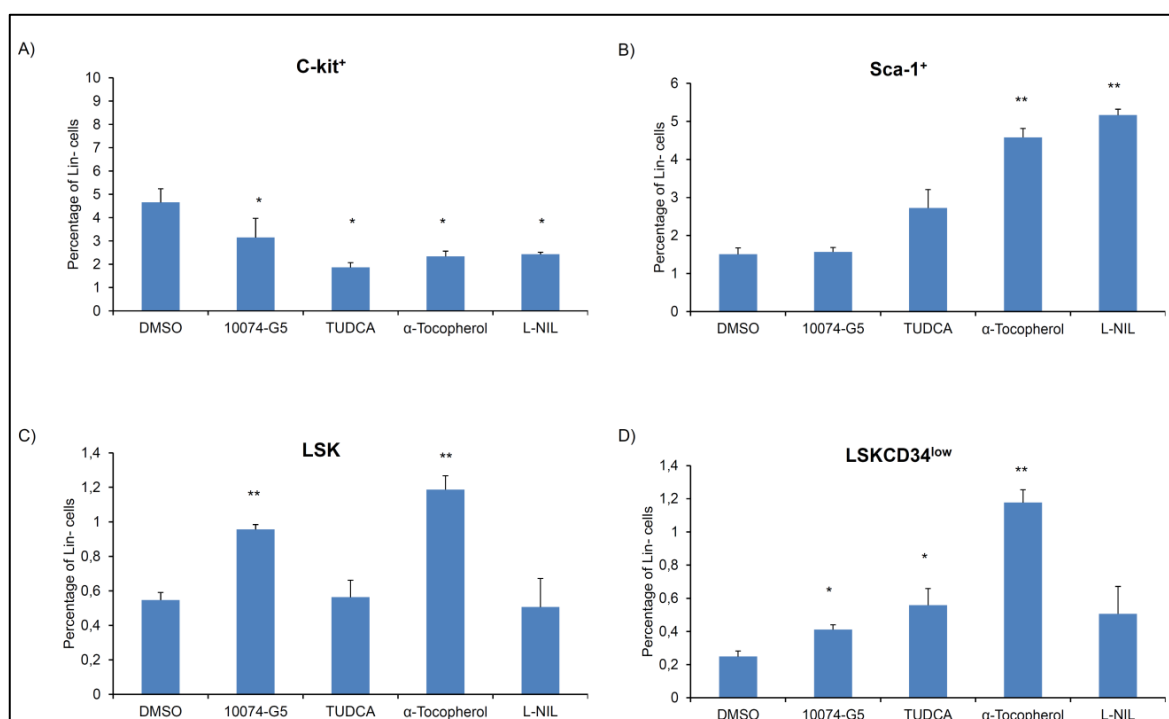


Figure 3.1. Effect of C-myc inhibition on murine HSCs. Mouse lin- cells have been treated with DMSO (control, 0.5%), 10074-G5 (c-myc inhibitor, 10  $\mu$ M), TUDCA (10  $\mu$ M),  $\alpha$ -Tocopherol (10  $\mu$ M), L-NIL (10  $\mu$ M) for 7 days and determined percent of A) C-Kit, B) Sca-1, C) Lin<sup>-</sup>Sca1<sup>+</sup>C-Kit<sup>+</sup> (LSK), D) Lin<sup>-</sup>Sca1<sup>+</sup>C-Kit<sup>+</sup>CD34<sup>Low</sup> (LSKCD34<sup>low</sup>). Note that c-myc inhibition significantly increases LSK content. \*  $p < 0.05$ , \*\*  $p < 0.01$ .  $n=3$ .

To whether test 10074-G5 and other selected small molecules increase human HSCs, we treated human umbilical cord blood mononucleated cells with DMSO control (0.5%) and three different concentrations of HSMs as final concentrations of 0.1  $\mu$ m, 1  $\mu$ m and 10  $\mu$ m. for 7 days. We found that c-myc inhibition increased human CD34<sup>+</sup> and CD133<sup>+</sup> HSPC cell count up to 2 fold compared to control as analyzed by flow cytometry (Figure 3.2A and 3.2B).

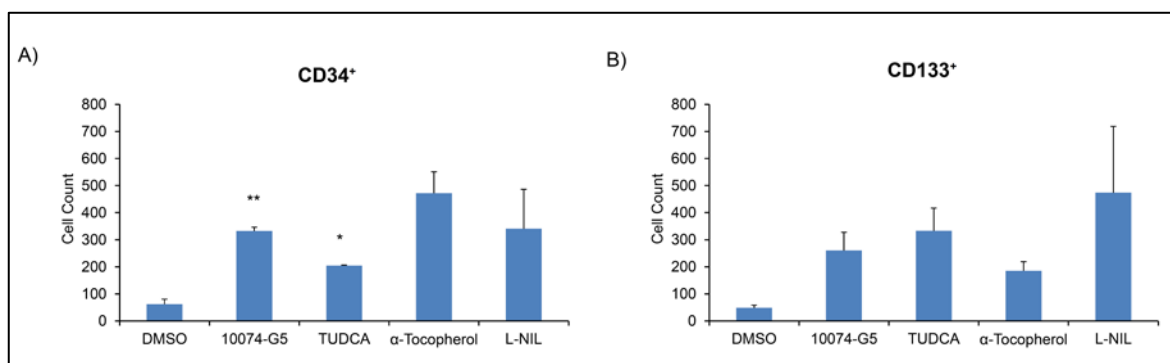


Figure 3.2. Effect of c-myc inhibition on human HSPCs. Human UCB cells have been treated with DMSO (control, 0.5%) and 0,1  $\mu$ M, 1  $\mu$ M, 10  $\mu$ M concentrations of 10074-G5 (c-myc inhibitor), TUDCA,  $\alpha$ -Tocopherol, L-NIL for 7 days and determined cell count of A) CD34+, B) CD133+ by flow cytometry. Note that c-myc inhibition significantly increases CD34+ cell count. \*  $p < 0.05$ , \*\*  $p < 0.01$ .  $n=3$ .

Apart from this, HSM treated lin<sup>-</sup> cells were stained with Hoechst 33342 and counted. The numbers showed that 10074-G5 increased the hematopoietic cell count compared to DMSO control (Figure A.1). To address increased HSPC frequency in murine, we first examined the cell cycle of LSK (Lin<sup>-</sup>Sca1<sup>+</sup>Ckit<sup>+</sup>) cells by using Hoechst 33342 and Pylonin Y staining. We found that increased HSPC proliferation was also evident by decreased murine HSPC content in Go phase of the cell cycle (Figure 3.3A and A.4). Cell cycle analysis showed that only around 3.17% DMSO treated HSPCs were in G1 compartment which is lower than that of 10074-G5, TUDCA,  $\alpha$ -Tocopherol and L-NIL treated HSPCs around 4.5%, 11.5%, 11.8%, 19.2% respectively (Figure 3.3B and A.4). This indicated that HSM treated HSPCs were much less quiescent and prone to proliferation. Next, we examined apoptosis status of LSK (Lin<sup>-</sup>Sca1<sup>+</sup>Ckit<sup>+</sup>) cells by using Annexin V and Propidium iodide (PI). We did not detect any significant apoptotic cells in 10074-G5, TUDCA,  $\alpha$ -Tocopherol and L-NIL treated HSPCs (Figure 3.4 and A.5).

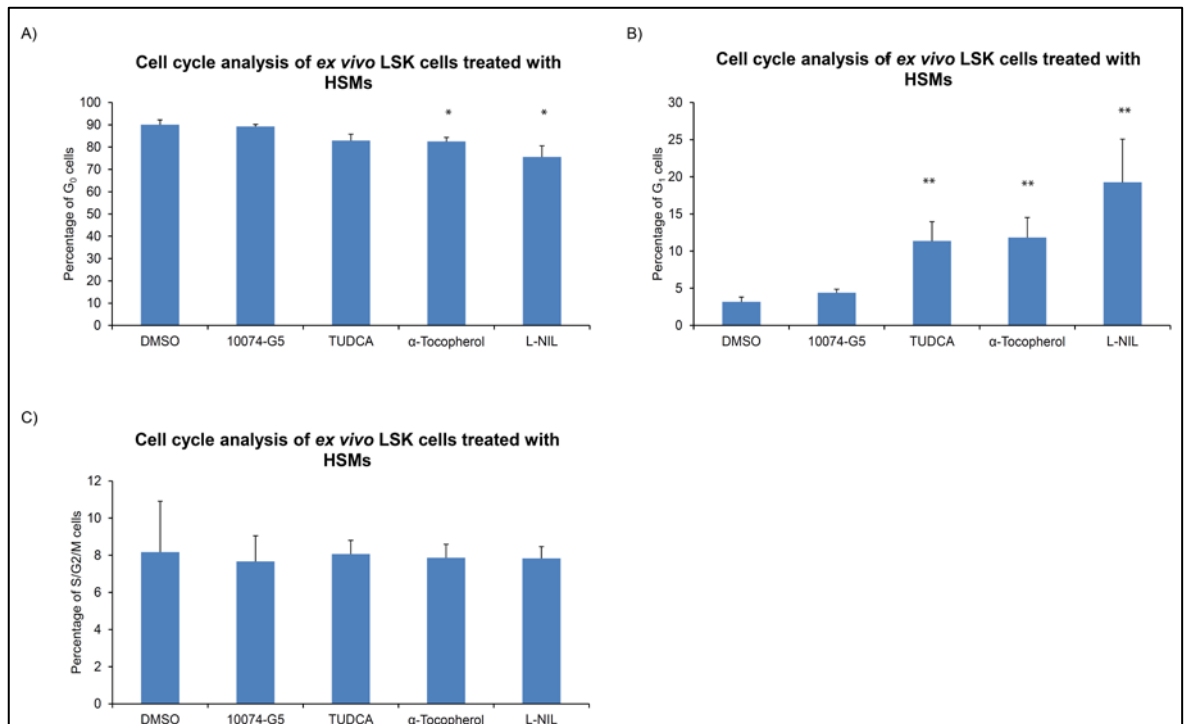


Figure 3.3. Cell cycle analysis of murine Lin<sup>-</sup>Sca1<sup>+</sup>C-Kit<sup>+</sup> (LSK) cells after HSM treatments. Murine LSK cells have been treated with DMSO (0.5%), 10074-G5 (c-myc inhibitor, 10  $\mu$ M), TUDCA (10  $\mu$ M),  $\alpha$ -Tocopherol (10  $\mu$ M), L-NIL (10  $\mu$ M) for 3 days and determined percent of cells in A) G<sub>0</sub>, B) G<sub>1</sub>, C) S/G<sub>2</sub>/M. \*  $p < 0.05$ , \*\*  $p < 0.01$ .  $n=3$ .

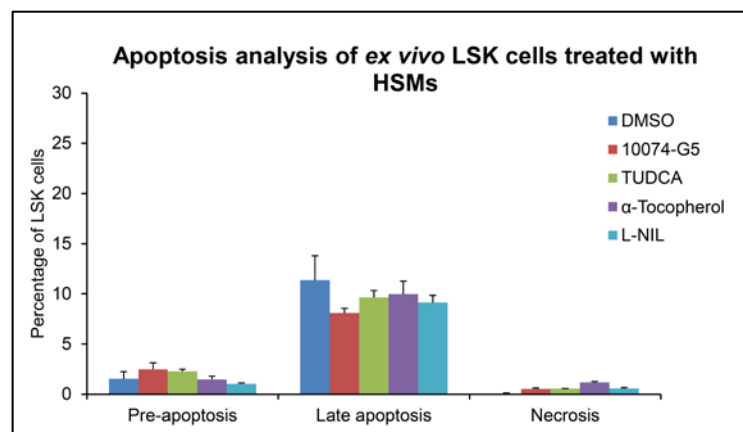


Figure 3.4. Apoptosis analysis of murine Lin<sup>-</sup>Sca1<sup>+</sup>C-Kit<sup>+</sup> (LSK) cells after HSM treatments. Murine LSK cells have been treated with DMSO (control, 0.5%), 10074-G5 (c-myc inhibitor, 10  $\mu$ M), TUDCA (10  $\mu$ M),  $\alpha$ -Tocopherol (10  $\mu$ M), L-NIL (10  $\mu$ M) for 3 days followed by staining with Annexin V FITC and propidium iodide and determined percent of live, pre-apoptotic, late apoptotic and necrotic cells.  $n=3$ .

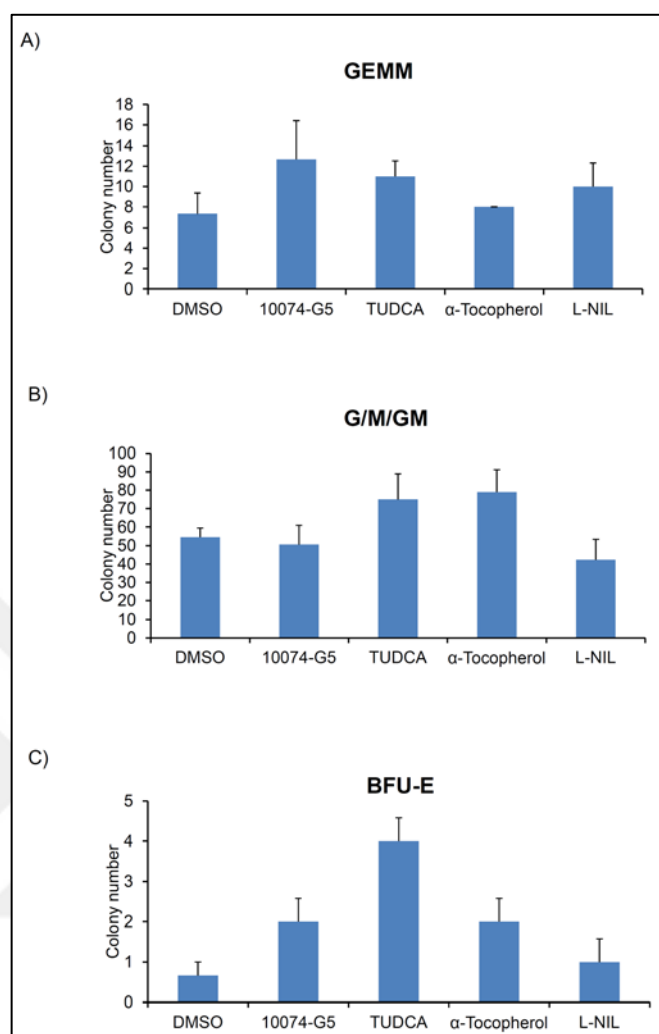


Figure 3.5. Colony-formation assay for lineage negative cells. Murine lineage negative cells have been treated with DMSO (control, 0.5%), 10074-G5 (c-myc inhibitor, 10  $\mu$ M), TUDCA (10  $\mu$ M),  $\alpha$ -Tocopherol (10  $\mu$ M), L-NIL (10  $\mu$ M) for 7 days in culture, then methylocellulose colony-forming assays were performed. Number of A) GEMM, B) G/M/GM, C) BFU-E colonies determined. \*  $p < 0.05$ , \*\*  $p < 0.01$ .  $n=3$ .

CFU-GEMM colonies representing most undifferentiated progenitors type of colonies derived from 10074-G5, TUDCA,  $\alpha$ -Tocopherol and L-NIL treated lineage negative cells. By using colony-forming assay, we demonstrated that 10074-G5 treated lineage negative cells had higher number of primitive myeloid progenitor cells (CFU-GEMM) and erythroid progenitor cells (BFU-E) compared to DMSO control but no significant change in number of differentiated myeloid progenitor cells after thirteen days of methocult assay. (CFU-GM) (Figure 3.5) .

### 3.2. EFFECT OF *IN VIVO* C-MYC INHIBITION ON HEMATOPOIETIC STEM CELLS

Direct *in vivo* targeting of HSCs could provide a physiological approach to modulate HSC activity as an alternative to HSC isolation and *ex vivo* expansion. *In vivo* injection of HSMs could play a molecular switch for expansion and mobilization of HSCs by inhibiting HSC quiescence regulators. In this aim, 10074-G5 was injected as three doses to adult wild type mice intraperitoneally. After three doses of treatment, stem cell expansion and stem cell mobilization were examined by flow cytometry following staining of bone marrow cells with alternative HSC surface antigens. As a result, we determined increase in Lin<sup>-</sup>CD48<sup>-</sup>, Lin<sup>-</sup>CD48<sup>-</sup>Sca1<sup>+</sup> and Lin<sup>-</sup>Sca1<sup>+</sup>Ckit<sup>+</sup>CD48<sup>-</sup>CD150<sup>+</sup> (LSKCD48<sup>-</sup>CD150<sup>+</sup>) compartments. The HSC pool in bone marrow, LSKCD48<sup>-</sup>CD150<sup>+</sup> compartment, increased to 0.064% compared to DMSO control 0.027% (Figure 3.6). Moreover, to measure HSC mobilization peripheral blood was collected through retroorbital bleeding and LSK and LSKCD34<sup>low</sup> cells quantified by flow cytometry analysis. However, we did not detected significant increase in the enrichment of both compartments after *in vivo* injection of 10074-G5 compared to control. Incidence of LSK cells was 0.18% and LSKCD34<sup>low</sup> was 0.16% when DMSO was injected, in comparison to 10074-G5 injection 0.23% and 0.19%, respectively (Figure 3.7). The results suggested that expanded HSC pool in BM was evident *in vivo* effect of 10074-G5.

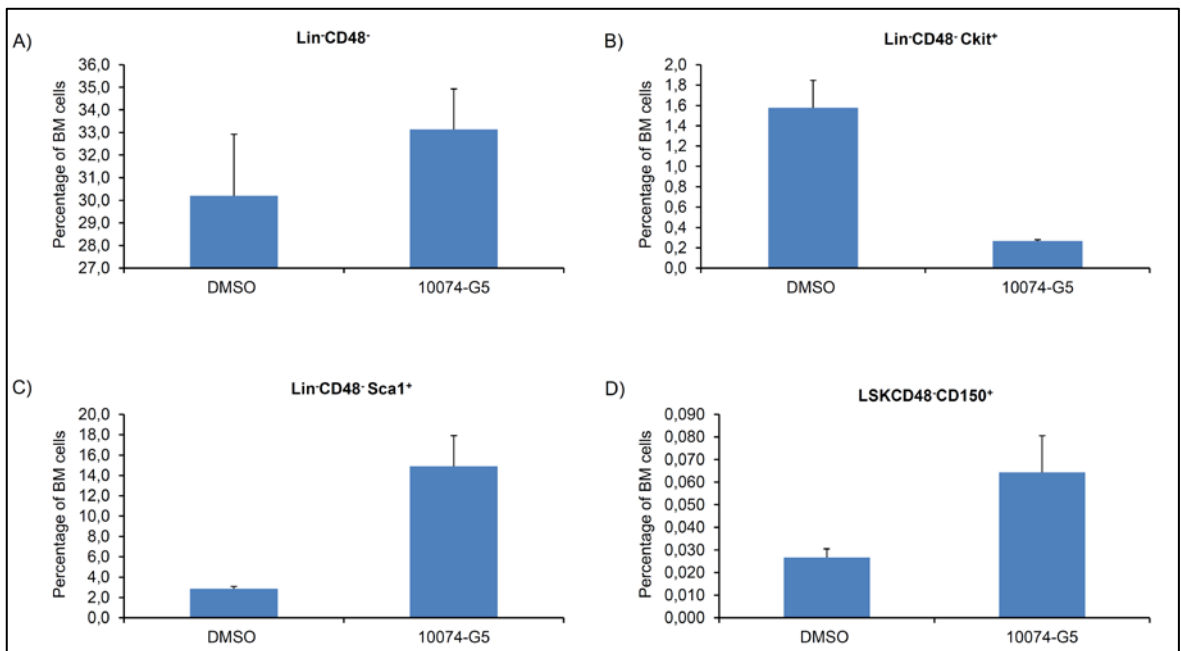


Figure 3.6. *In vivo* c-myc inhibition increased frequency of HSC compartments on murine bone marrow cells. Percent of A) Lin<sup>-</sup>CD48<sup>-</sup>, B) Lin<sup>-</sup>CD48<sup>-</sup>CKit<sup>+</sup>, C) Lin<sup>-</sup>CD48<sup>-</sup>Sca1<sup>+</sup> D) Lin<sup>-</sup>Sca1<sup>+</sup>C-Kit<sup>+</sup>CD48<sup>-</sup>CD150<sup>+</sup>. n=3.

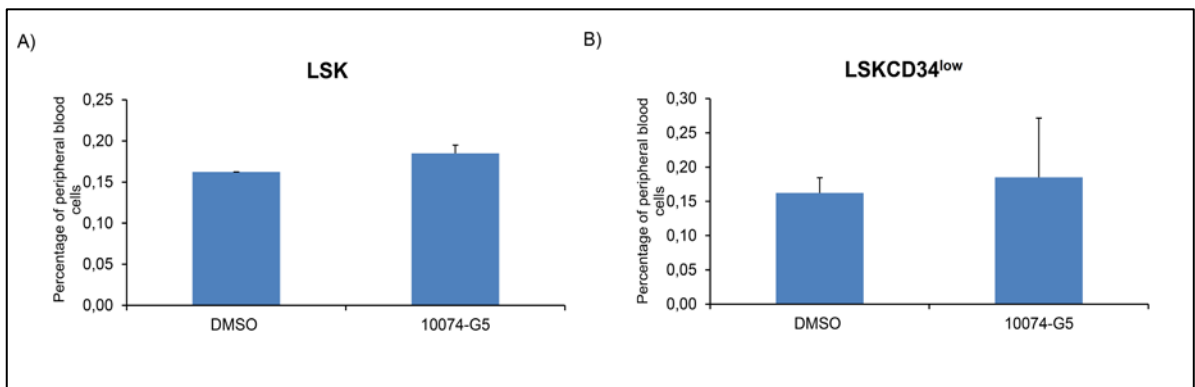


Figure 3.7. *In vivo* c-myc inhibition increased mobilization of HSCs to peripheral blood. Incidence of A) Lin<sup>-</sup>Sca1<sup>+</sup>C-Kit<sup>+</sup> (LSK) B) Lin<sup>-</sup>Sca1<sup>+</sup>C-Kit<sup>+</sup>CD34<sup>low</sup> following three doses of *in vivo* treatments.

### 3.3. C-MYC INHIBITION INHIBITS BM-MSCS PROLIFERATION BUT DO NOT CHANGE PROLIFERATION KINETICS OF AD-MSCS, HUVECS OR HDFs

There are two stem cell populations that reside in adult bone marrow: hematopoietic stem cells and mesenchymal stem cells. We showed that c-myc inhibitor, 10074-G5, increased murine and human hematopoietic stem and progenitor cells. Next, we sought to determine the effect of 10074-G5 and other HSMs on murine bone marrow and human adipose derived mesenchymal stem cells. Cell proliferation was determined using the WST1 assay after three days of HSM treatment. The results showed that c-myc inhibitor 10074-G5 and other HSMs decreased the proliferative rate of BM-MSCs (Figure 3.8A). However, we did not detect any significant change in proliferation of AD-MSCs compared to control (Figure 3.8B). These results suggest that c-myc inhibitor and other HSMs do not change proliferation kinetics of AD-MSCs but intriguingly they suppress the proliferation of BM-MSCs.

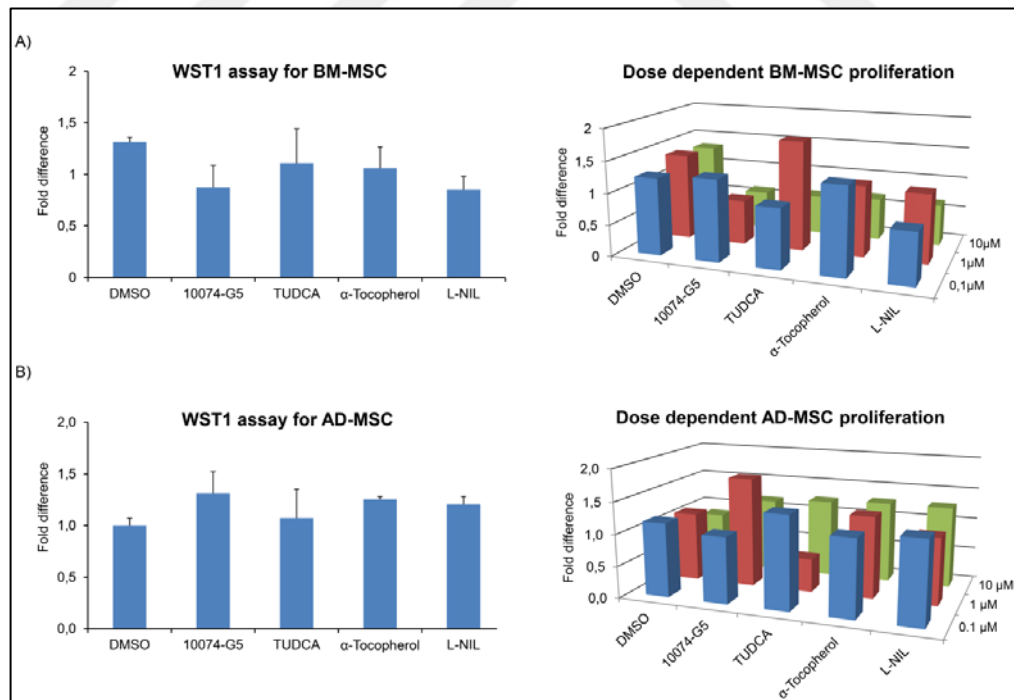


Figure 3.8. Effect of 10074-G5 on BM-MSC and AD-MSC proliferation. A) Murine BM-MSCs and B) human AD-MSCs were treated with DMSO (control, 0.5%) and 0,1 $\mu$ M, 1  $\mu$ M, 10  $\mu$ M concentrations of 10074-G5, TUDCA,  $\alpha$ -Tocopherol, L-NIL for 3 days and proliferation then examined by using WST1 assay. Absorbance at 450 nm was plotted.

To see c-myc inhibitor' effect on proliferation of different cell lines, we treated human vascular endothelial cells and dermal fibroblasts with three different concentrations of (0.1  $\mu$ M, 1 $\mu$ M and 10 $\mu$ M) 10074-G5 and other HSMs. 10074-G5 treated HUVECs (Figure 3.9A) and HDFs (Figure 3.9B) showed no difference in proliferation compared to control. Taken together, these results indicated that c-myc inhibitor, 10074-G5, only specific to induction of hematopoietic stem and progenitor cells.

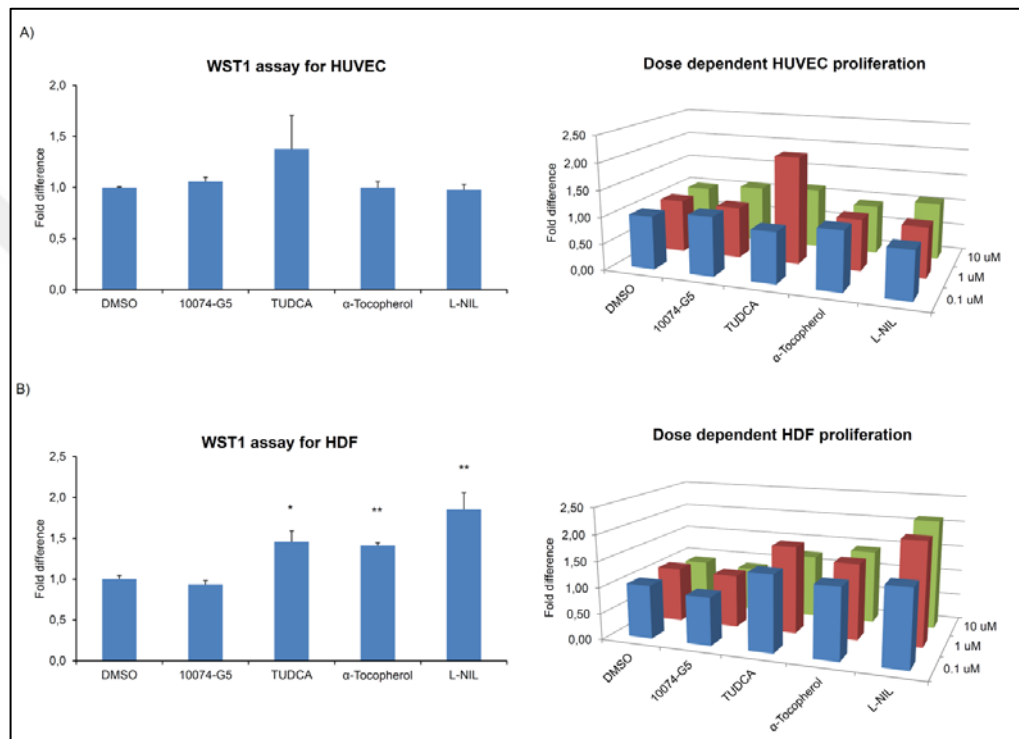


Figure 3.9. C-myc inhibition do not affect proliferation of human endothelial cell or dermal fibroblast proliferation. A) HUVECs and B) HDFs were treated with DMSO (control, 0.5%) and 0,1 $\mu$ M, 1  $\mu$ M, 10  $\mu$ M concentrations of 10074-G5 (C-myc inhibitor), TUDCA,  $\alpha$ -Tocopherol, L-NIL for 3 days and proliferation then examined by using WST1 assay.

Absorbance at 450 nm was plotted.

#### 3.4. ANALYSIS OF C-MYC TARGET GENE EXPRESSION PROFILE POST TREATMENT WITH 10074-G5

In the present study, we demonstrated that c-myc inhibitor increased the percentage of  $G_0$  to  $G_1$  transition of hematopoietic stem and progenitor cells (Figure 3.3). Moreover, along with *in vivo* studies we strengthen our hypothesis and indicated that percent of LSKCD48<sup>+</sup>

CD150<sup>+</sup> cells were increased after 10074-G5 injection as analyzed by flow cytometry (Figure 3.6). We confirmed this by examining the mRNA levels of cell cycle inhibitors after *in vitro* treatment and *in vivo* injection of c-myc inhibitor, 10074-G5. Furthermore, we analyzed c-myc target gene expressions following *in vitro* and *in vivo* treatments with 10074-G5 to understand how c-myc contribute to expansion of hematopoietic stem and progenitor cells. In the first place, we sought to determine c-myc gene expression profile in whole bone marrow (WBM) cells, lineage negative cells and HSCs (LSKCD34<sup>low</sup>) of wild type mouse. The results showed that c-myc expressed in hematopoietic stem and progenitor cells (Figure 3.10).

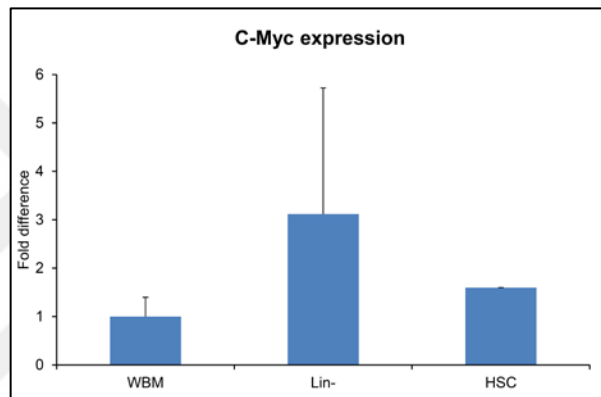


Figure 3.10. The expression analysis of C-Myc in whole bone marrow (WBM), lineage negative cells (Lin-) and hematopoietic stem cells (HSCs). Note that  $\beta$ -actin was used as a housekeeping control. n=2.

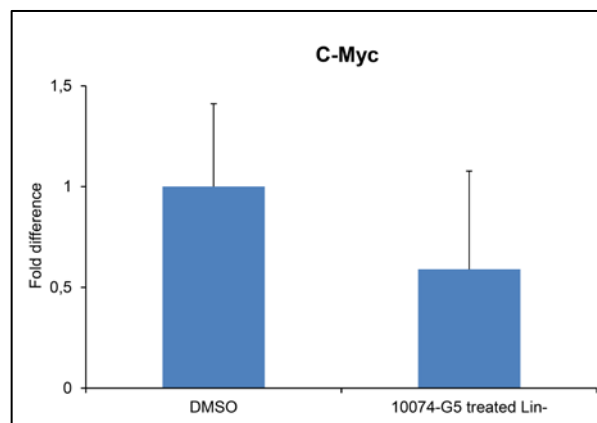


Figure 3.11. *In vitro* treatment of lineage negative cells with 10074-G5 downregulates transcription of C-myc. Note that  $\beta$ -actin was used as a housekeeping control. n=2.

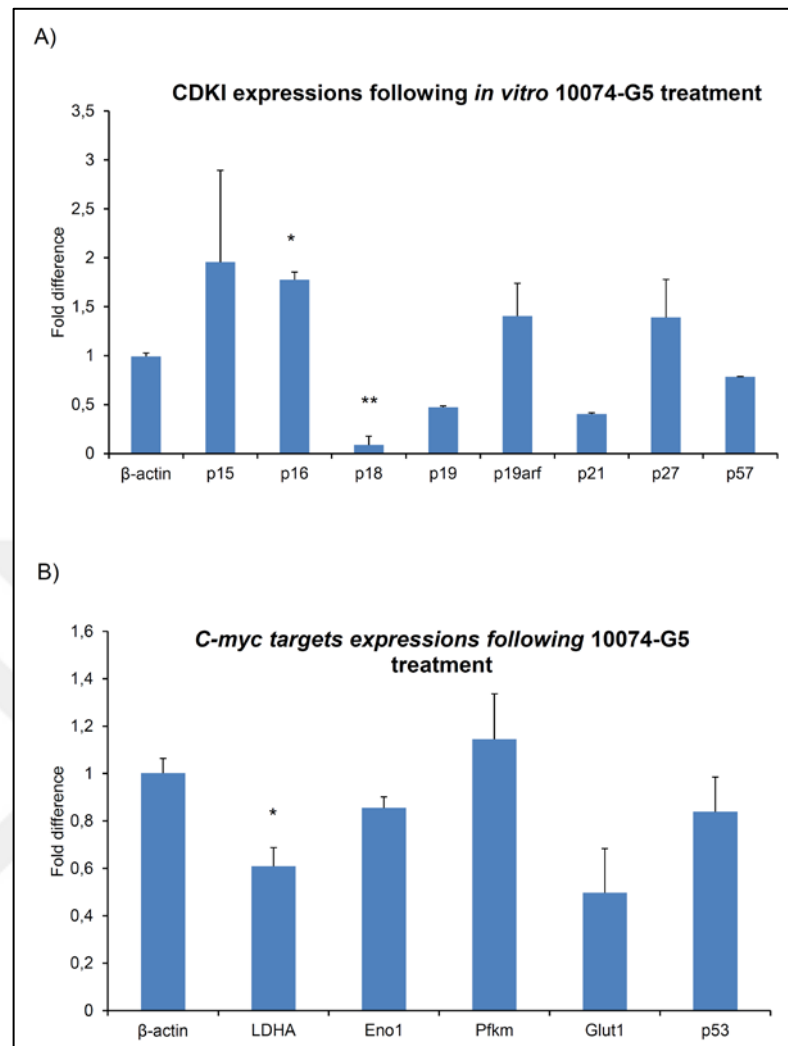


Figure 3.12. *In vitro* treatment of lineage negative cells with 10074-G5 downregulates transcription of A) Cyclin dependent kinase inhibitors (CDKIs) and B) C-myc targets.

Note that  $\beta$ -actin was used as a housekeeping control. n=2.

Next, we examined c-myc gene and cell cycle inhibitors expression profile after *in vitro* treatment with c-myc inhibitor. Lineage negative cells were treated with 10074-G5 at a concentration of 10  $\mu$ M and DMSO control (%0.5) for 5 days in humidified incubator at 37°C and 5% CO<sub>2</sub>. Then, transcription of c-myc gene, cell cycle inhibitors and c-myc targets were analyzed by using Real-time PCR. The results demonstrated that expression of c-myc decreased when it was treated with 10074-G5 in comparison to DMSO control (Figure 3.11). Expression level of cell cycle inhibitors which are p18 (CDKN2C), p19 (CDKN2D), p21<sup>CIP1</sup> (CDKN1A), p57<sup>KIP2</sup> (CDKN1C) was declined (Figure 3.12A). Additionally, transcription of some of c-myc targets which are LDHA, Eno1, Glut1 and p53 were decreased (Figure 3.12B).

In the second place, we detected mRNA levels of cell cycle inhibitors and c-myc target genes in bone marrow by using RT-PCR following *in vivo* injection of c-myc inhibitor, 10074-G5. The mRNA levels of p15<sup>INK4B</sup> (CDKN2B), p16<sup>INK4A</sup>, p19<sup>ARF</sup>, p21<sup>CIP1</sup> (CDKN1A), p27<sup>KIP1</sup> (CDKN1B) and p57<sup>KIP2</sup> (CDKN1C) downregulated while transcription of p18 (CDKN2C) and p19 (CDKN2D) increased (Figure 3.13A). C-myc targets, which are energy metabolism genes LDHA, Eno1, HK2, Pfkf, Glut1 and apoptosis related p53 were studied in the context of downstream of c-myc. Expression of Eno1, HK2, Pfkf and Glut1 was declined however, LDHA and p53 did not show any significant change (Figure 3.13B).

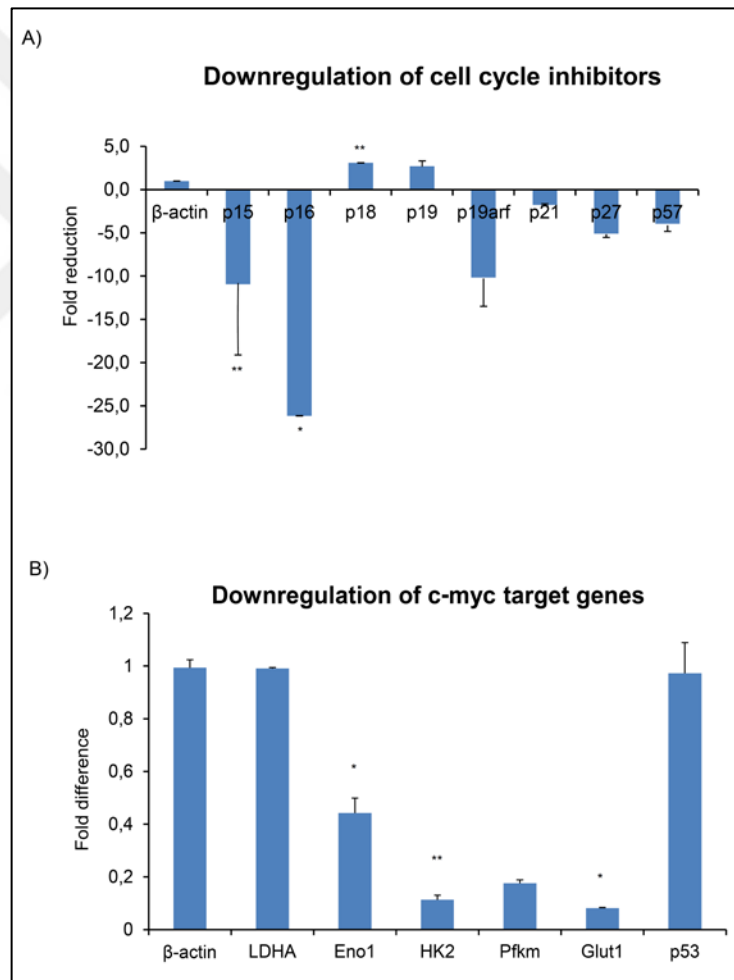


Figure 3.13. *In vivo* injection of 10074-G5 downregulates the transcription of genes that are downstream of c-myc. After three dose-repeat *in vivo* injection of 10074-G5, mice were euthanized and bone marrow cells were analyzed for transcription of A) cell cycle inhibitors B) c-myc target genes. Note that  $\beta$ -actin was used as a housekeeping gene, DMSO was used as a control. \*  $p < 0.05$  \*\* $p < 0.01$ . n=2.

### 3.5. INHIBITION OF C-MYC ALLOWS DEVELOPMENT OF *EX VIVO* HSC EXPANSION COCKTAIL

We also hypothesized that an optimum combination of HSMs could provide a robust HSC expansion by targeting several pathways. In order to determine optimum combination of HSMs, we performed flow cytometry analysis following by staining with hematopoietic stem cell markers ( $\text{Lin}^- \text{Sca1}^+ \text{Kit}^+ \text{CD34}^-$ ). The results of this analysis demonstrated that c-myc inhibitor 10074-G5 along with other HSMs (M5, M6, M7, M11, M12, M13, M14) yielded superior expansion of HSPCs (Figure 3.14).

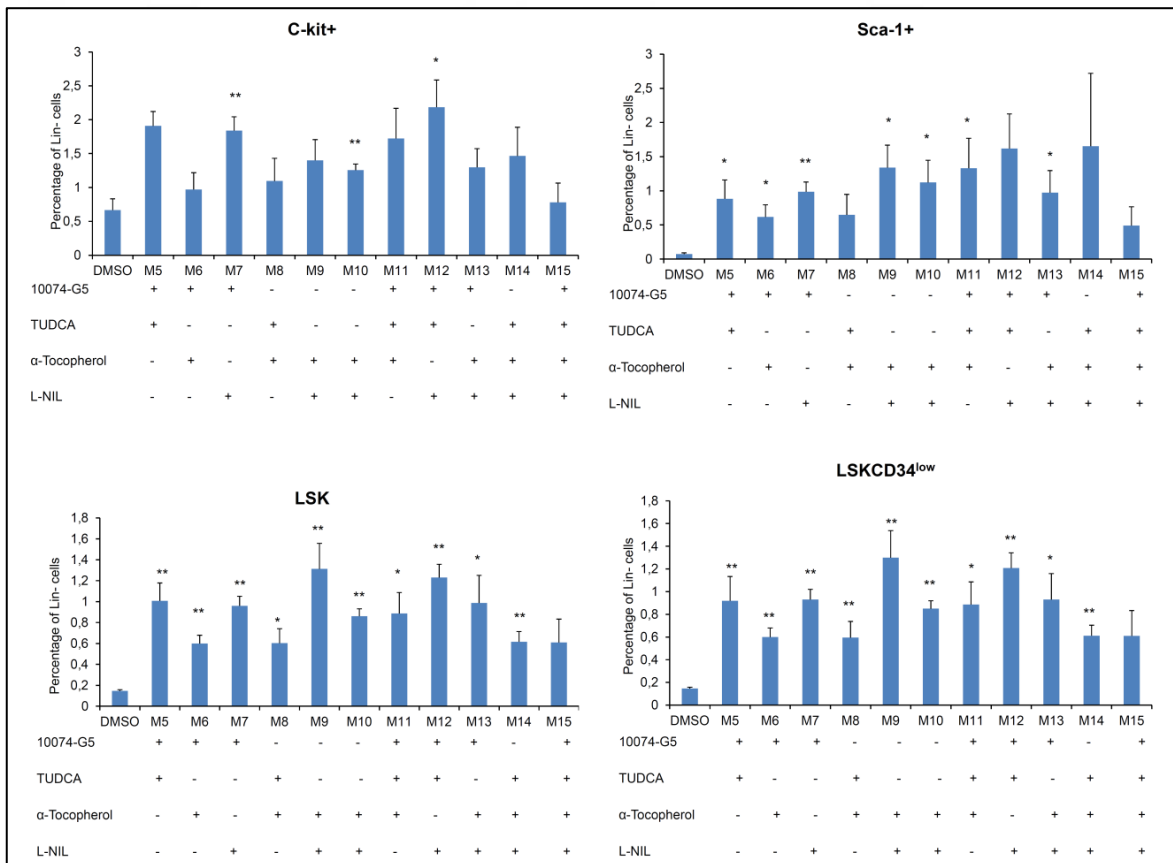


Figure 3.14. Combining C-myc inhibitor, 10074-G5, with other HSMs allows robust *ex vivo* expansion of HSPCs. Mouse lin<sup>-</sup> cells have been treated with DMSO (control, 0.5%) and combination of 10074-G5, TUDCA, α-Tocopherol, L-NIL for 7 days and determined percent of A) C-Kit, B) Sca-1, C)  $\text{Lin}^- \text{Sca1}^+ \text{C-Kit}^+$  (LSK), D)  $\text{Lin}^- \text{Sca1}^+ \text{C-Kit}^+ \text{CD34}^{\text{Low}}$  (LSKCD34<sup>low</sup>). \*  $p < 0.05$ , \*\*  $p < 0.01$ .  $n=3$ .

## 4. DISCUSSION

Hematopoietic stem cells are defined by their inherent capacity to self-renew, that relies on the ability of a small number of HSCs, and to differentiate into any blood cell types [4]. They primarily maintained in a quiescent state within particular bone marrow-microenvironment known as a niche. HSCs involve in active phases of cell cycle in response to cell-intrinsic and cell-extrinsic stimulus thus undergoing self-renewal divisions or differentiation [76]. The primarily therapeutic modality for many hematopoietic disorders such as leukemia, lymphoma and autoimmune disorders is bone marrow transplantation. Sufficient number of HSCs is needed for effective transplantation and engraftment. This needs expansion of functional HSCs which is safe to recipient. Many studies addressed to define *ex vivo* culture conditions which relies on cytokines and growth factors to expand functional HSCs, however HSC expansion by utilizing small molecules that targets HSC quiescence regulators have not been widely studied. Kocabas and colleagues have shown that HSCs expanded *in vivo* after stem cell specific knockout of hematopoietic factors for instance Meis1 and Hif-1 $\alpha$  [13]. Deletion of such HSC quiescence related factors in HSC compartment not only leads to cell cycle entry but also provide HSC expansion. Thereby, we hypothesized that treatment of HSCs with putative HSMs could stimulate *ex vivo* expansion of HSCs.

Using small molecule databases, we have identified 4 putative hematopoietic small molecules (HSM) targeting 4 hematopoietic factors, 3 of which (TUDCA,  $\alpha$ -Tocopherol and L-NIL) , have already been shown to expand HSCs *in vitro* or *in vivo* [73, 74, 72]. Wilson et al. showed that lineage negative cell population was 3-fold increased 3 week after *in vivo* c-myc deletion. Additionally, they illustrated two to threefold rise in the absolute number of KLS-HSCs (Ckit<sup>+</sup>Lin<sup>-</sup>Sca1<sup>+</sup>) [60]. Thus, targeting of HSC regulator c-myc using small molecule inhibitors may provide valuable tools for *ex vivo* or *in vivo* HSC expansion. Intriguingly, 10074-G5 has not been previously studied in small molecule induced *ex vivo* HSC expansion procedures. To this end, the effect of 10074-G5, TUDCA,  $\alpha$ -Tocopherol and L-NIL on *ex vivo* HSC expansion isolated from wild type adult mice was investigated. C-Myc inhibitor, 10074-G5, was significantly increased murine LSK and LSKCD34<sup>low</sup> compartment more than 1.5 fold (Figure 3.1 and A.2). The other tested HSMs also provided increase in LSKCD34<sup>low</sup> compartment. Moreover, when we treated human

UCB mononuclear cells with 10074-G5, c-myc inhibition increased human CD34<sup>+</sup> and CD133<sup>+</sup> HSPC cell count upto 2 fold compared to control as analyzed by flow cytometry (Figure 3.2). To address increased HSPC frequency in murine, we examined the cell cycle of LSK (Lin<sup>-</sup>Sca1<sup>+</sup>Ckit<sup>+</sup>) cells by using Hoechst 33342 and Pyronin Y staining. We found that increased HSPC proliferation was also evident by increased cycling. HSM treated HSPCs were much less quiescent and prone to proliferation (Figure 3.3). Next, apoptosis status of LSK cells was examined by using Annexin V and PI. We observed unaffected apoptotic cell rates in HSPCs treated with 10074-G5, TUDCA,  $\alpha$ -Tocopherol and L-NIL (Figure 3.4). In addition, CFU assays showed increased mixed colonies as a measure of increased number of functional hematopoietic stem and progenitor cell following 10074-G5 treatment (Figure 3.5). In previous studies, it has been showed that TUDCA treated-CD34<sup>+</sup>48<sup>-</sup>KSL increased total hematopoietic cell number and the percentage of CD34<sup>+</sup>48<sup>-</sup>KSL cells [72].  $\alpha$ -Tocopherol-injected mice, showed increase in the c-Kit<sup>+</sup>, LSK, and HP populations [73]. Treatment with the selective iNOS inhibitor, L-NIL, increased preservation of human CD34<sup>+</sup> progenitors [74]. Total human CD34<sup>+</sup> cell number 4-fold expanded with a hematopoietic cytokine cocktail in contrast to 5.2-fold with addition of L-NIL to the combination [74]. Thus, in this present study, we also confirmed the expansion of HSCs by using TUDCA,  $\alpha$ -tocopherol and L-NIL with our findings and suggested that TUDCA,  $\alpha$ -tocopherol and L-NIL are functional on *ex vivo* HSC expansion.

Direct *in vivo* targeting of HSCs could provide a physiological approach to modulate HSC activity as an alternative to HSC isolation and *ex vivo* expansion. *In vivo* injection of HSMs could play a molecular switch for expansion and mobilization of HSCs by inhibiting HSC quiescence regulators. After HSM treatment, stem cell expansion and stem cell mobilization were analyzed by flow cytometry in bone marrow and peripheral blood of murine. LSKCD48<sup>-</sup>CD150<sup>+</sup> compartment in bone marrow increased 2.3 fold compared to DMSO control (Figure 3.6). In peripheral blood, there was only about 1.2 fold increase in LSK and LSKCD34<sup>low</sup> cells (Figure 3.7). Enriched HSC pool in bone marrow was evident *in vivo* effect of 10074-G5. HSC mobility in blood was not affected. However, further experiments are needed to show increased cycling and functional HSCs for *in vivo* experiments.

Two stem cell populations located in adult bone marrow: hematopoietic stem cells and mesenchymal stem cells. We demonstrated that c-myc inhibitor, 10074-G5, increased

murine and human hematopoietic stem and progenitor cells. Next, we sought to determine the effect of 10074-G5 and other HSMs on murine bone marrow and human adipose derived mesenchymal stem cells. 10074-G5 and other HSMs inhibited the proliferation of BM-MSCs (Figure 3.8A) however did not show any effect on proliferation of AD-MSCs (Figure 3.8B). However, to determine the effect of 10074-G5 and other HSMs on proliferation of different cell lines, human vascular endothelial cells and dermal fibroblasts were treated with selected HSMs. 10074-G5 treated HUVECs (Figure 3.9A) and HDFs (Figure 3.9B) showed no difference in proliferation compared to control. Taken together, these results indicate that c-myc inhibitor, 10074-G5, only specific to induction of hematopoietic stem and progenitor cells.

C-Myc gene is involved in glycolysis owing to the detection of LDHA, which generate lactate from pyruvate as part of the glycolytic pathway [43, 42]. Several glucose metabolism genes are also directly regulated by c-Myc, including GLUT1, PFKM, HK2, ENO1 [44-47]. Through the upregulation of these downstream targets, c-myc induces the Warburg effect which enables generation of pyruvate from glucose even under adequate oxygen tension. Besides, p53 tumor suppressor protein was shown to regulate mitochondrial function and glycolysis in which its absence is linked with elevated aerobic glycolysis [49]. Myc controls cell cycle progress by activating cyclins and elimination of cell cycle checkpoints also inhibition of the CDKIs [55]. A number of stem cells have been indicated to reside in their hypoxic niches, which suggest presence of special metabolic adaptations for stem cells [10]. Nevertheless, metabolic phenotype and how metabolism of stem cells is related to their cell cycle have not been widely known [11, 12]. Therefore, we set out to outline the link between metabolism and cell cycle regulation of stem cells. In the present study, it has been demonstrated that c-myc inhibitor increased the percentage of  $G_0$  to  $G_1$  transition of hematopoietic stem and progenitor cells (Figure 3.3). Moreover, along with *in vivo* studies we strengthen our hypothesis by indicating that percent of LSKCD48<sup>+</sup>CD150<sup>+</sup> cells in bone marrow and LSKCD34<sup>low</sup> cells in peripheral blood were increased after 10074-G5 injection as analyzed by flow cytometry (Figure 3.6 and 3.7). To discover how stem cells can contribute to expansion, cell cycle inhibitors and downstream target genes of c-myc were studied in this context. First, we detected expression of c-myc in whole bone marrow, lineage negative cells and HSCs by RT-PCR (Figure 3.10). Second, expression of C-myc, CDKI and C-myc targets were analyzed after *in vitro*

treatment with c-myc inhibitor. The results demonstrated that expression of c-myc was declined in 10074-G5 treated cells in comparison to DMSO control (Figure 3.11). Expression level of cell cycle inhibitors which are p18, p19, p21<sup>CIP1</sup>, p57<sup>KIP2</sup> and c-myc targets LDHA, Eno1, Glut1 and p53 were decreased (Figure 3.12). The last but not the least, *in vivo* bone marrow cells were analyzed for same targets. The mRNA levels of cell cycle inhibitors, p15<sup>INK4B</sup>, p16<sup>INK4A</sup>, p19<sup>ARF</sup>, p21<sup>CIP1</sup>, p27<sup>KIP1</sup>, p57<sup>KIP2</sup> and c-myc downstream genes Eno1, HK2, Pfkf and Glut1 was downregulated (Figure 3.13). These suggested that expansion of HSCs could be related to inhibition of cell cycle inhibitors or through downregulation of glucose metabolism genes.

Targeting of a single pathway or gene may lead to HSC senescence. In addition, HSC expansion procedures may result in HSC dormancy and exhaustion due to increased expression of quiescence genes. Thus, we hypothesized that mixture of HSMs could provide a superior HSC expansion by targeting several pathways. In this aim, various combinations of selected four small molecules have been tested. The results of this analysis demonstrated that c-myc inhibitor 10074-G5 along with other HSMs yielded superior expansion of HSPCs.

In this study, some of anticipated results could arise due to toxicity of the compounds, differentiation during expansion and loss of HSC surface markers used in flow cytometry analysis. This study addresses identification of a novel small molecule, 10074-G5 in HSC expansion procedures. We expected to see higher number of HSCs following passages compared to DMSO control and lower or unchanged apoptotic cell rates with hematopoietic small molecule tested. Additionally, increased mixed colonies (CFU-GEMM) as a measure of increased number of functional HSPCs was expected in this context. Based on our hypothesis, frequency of HSCs needed to change in HSM treated mice. Based on our results, we conclude that 10074-G5 could be used for *ex vivo* HSC expansion.

## 5. CONCLUSION

Under steady state, HSCs are maintained quiescent within the stem cell niche in the BM [72]. The balance between quiescence and proliferation of HSCs is strictly controlled to maintain homeostasis and ensure HSCs lifelong [17]. HSCs' ability to proliferate is restricted in culture compared to their strong capacity *in vivo*. To expand HSCs for clinical use, specific hematopoietic growth factors have been used or cells were induced by specific HSC regulators *in vitro*. The elucidation of specific HSC regulators revealed limited number of genes that play major role in self-renewal of HSCs. Small molecules that target quiescence factors involved in HSC quiescence have not been widely used for expansion of HSCs. We anticipate that hematopoietic small molecules will bring new approaches to the expansion of HSCs in cell culture. Using small molecule databases, we have identified 4 putative hematopoietic small molecules targeting 4 hematopoietic factors, 3 of which (TUDCA,  $\alpha$ -Tocopherol and L-NIL), have already been shown to expand HSCs *in vitro* or *in vivo*. Intriguingly, c-myc inhibitor, 10074-G5 has not been previously studied in small molecule induced *ex vivo* HSC expansion procedures.

In this study, murine HSPCs were treated with 10074-G5, TUDCA,  $\alpha$ -Tocopherol and L-NIL. We found that, 10074-G5 and tested HSMs led to about 2-fold increase in murine LSKCD34<sup>low</sup> compartment post 7 days of treatment. To address increased HSPC frequency in murine, we examined the cell cycle of LSK cells by using Hoechst 33342 and Pyronin Y staining. Increased HSPC proliferation was also evident by decreased murine HSPC content in Go phase of the cell cycle. Moreover, CFU assays showed increased mixed colonies as a measure of increased number of functional hematopoietic stem and progenitor cell following 10074-G5 treatment. Furthermore, when we treated human UCB cells with 10074-G5, c-myc inhibition increased human CD34+ and CD133+ HSPC cell count upto 2 fold compared to control as analyzed by flow cytometry.

Next, we sought to determine the effect of 10074-G5 and other HSMs on murine bone marrow and human adipose derived mesenchymal stem cells. C-myc inhibition inhibits bone marrow derived mesenchymal stem cell expansion but does not alter proliferation kinetics of adipose derived mesenchymal stem cells, endothelial cells or fibroblasts.

LSKCD48-CD150<sup>+</sup> compartment in bone marrow increased 2.3 fold *in vivo* after 10074-G5 injection compared to DMSO control indicating enriched HSC pool in BM. However, HSC mobility in peripheral blood was not affected after *in vivo* injection of 10074-G5.

To discover how stem cells can contribute to expansion, cell cycle inhibitors and downstream target genes of c-myc were studied in this context. Myc controls cell cycle progress by activating cyclins and inhibition of the CDKIs. C-Myc targets and cell cycle inhibitors were downregulated after *in vitro* and *in vivo* treatments. Our results suggested that expansion of HSCs could be related to inhibition of cell cycle inhibitors or through downregulation of glucose metabolism genes. The last but not the least, we hypothesized that mixture of HSMs could provide a robust HSC expansion by targeting several pathways. In this aim, different combinations of selected four small molecules have been tested. 10074-G5 along with TUDCA and L-NIL (M12 mix) yielded superior expansion of HSPCs.

As a result, findings from the study suggest that c-myc inhibitor 10074-G5 and other HSMs, which are TUDCA,  $\alpha$ -Tocopherol and L-NIL are specific to induction of HSPCs proliferation rather than other cell types. Expansion of HSCs was evident in increase in HSC frequency, reduction of the number of HSCs in quiescent state. This study allowed us to identify hematopoietic factors and their corresponding small molecule inhibitors. Moreover, our study establish role of novel c-myc inhibitor, 10074-G5 in expansion of HSCs. 10074-G5 can be further exploited to increase *ex vivo* HPSC expansion and eventually transplantation efficiency.

## 6. FUTURE PROSPECTS

For future studies, HSC and progenitor fate will be analyzed to whether detect differentiation of hematopoietic stem cells. Competitive bone marrow transplantation assays are planned to show functional expansion of HSCs following HSM treatment. This will involve engraftment of HSC into NSG mice and analysis of incidence of donor-derived cells in bone marrow and their ability to repopulate whole bone marrow following serial bone marrow transplantations. Enriched HSC pool in bone marrow was evident *in vivo* effect of 10074-G5. However, further experiments are needed to show increased cycling and functional HSCs for *in vivo* experiments.

## REFERENCES

1. I.L. Weissman. Stem cells: Units of Development, Units of Regeneration and Units in Evolution. *Cell*, 100: 157-168, 2000.
2. R. Kumar, A. Sharma, A.K. Pattnaik and P.K. Varadwaj. Stem cells: An Overview with Respect to Cardiovascular and Renal Disease. *Journal of Natural Science, Biology, and Medicine*, 1: 43-52, 2010.
3. M. Soleimani and S. Nadri. A Protocol for Isolation and Culture of Mesenchymal Stem Cells from Mouse Bone Marrow. *Nature Protocols*, 4: 102-106, 2009.
4. F. Kocabas, L. Xie, J. Xie, Z. Yu, R.J. DeBerardinis, W. Kimura, S. Thet, A.F. Elshamy, H. Abouellail, S. Muralidhar, X. Liu, C. Chen, H.A. Sadek, C.C. Zhang and J. Zheng. Hypoxic Metabolism in Human Hematopoietic Stem Cells. *Cell and Bioscience*, 5: 39, 2015.
5. J. Seita and I.L. Weissman. Hematopoietic Stem Cell: Self-renewal Versus Differentiation. *Wiley Interdisciplinary Reviews Systems Biology and Medicine*, 2: 640-653, 2010.
6. L.M. Calvi, G.B. Adams, K.W. Weibrecht, J.M. Weber, D.P. Olson, M.C. Knight, R.P. Martin, E. Schipani, P. Divieti, F.R. Bringhurst, L.A. Milner, H.M. Kronenberg and D.T. Scadden. Osteoblastic Cells Regulate the Haematopoietic Stem Cell Niche. *Nature*, 425: 841-846, 2003.
7. J. Zhang, C. Niu, L. Ye, H. Huang, X. He, W.G. Tong, J. Ross, J. Haug, T. Johnson, J.Q. Feng, S. Harris, L.M. Wiedemann, Y. Mishina and L. Li. Identification of the Haematopoietic Stem Cell Niche and Control of the Niche Size. *Nature*, 425: 836-841, 2003.

8. F. Arai, A. Hirao, M. Ohmura, H. Sato, S. Matsuoka, K. Takubo, K. Ito, G.Y. Koh and T. Suda. Tie2/angiopoietin-1 Signaling Regulates Hematopoietic Stem Cell Quiescence in the Bone Marrow Niche. *Cell*, 118: 149-161, 2004.
9. F. Kocabas, J. Zheng, C. Zhang and H.A. Sadek. Metabolic Characterization of Hematopoietic Stem Cells. *Methods in Molecular Biology*, 1185: 155-164, 2014.
10. A. Mohyeldin, T. Garzon-Muvdi and A. Quinones-Hinojosa. Oxygen in Stem Cell Biology: A Critical Component of the Stem Cell Niche. *Cell Stem Cell*, 7: 150-161, 2010.
11. V. Aguilar and L. Fajas. Cycling Through Metabolism. *EMBO Molecular Medicine*, 2: 338-348, 2010.
12. M.R. Buchakjian and S. Kornbluth. The Engine Driving the Ship: Metabolic Steering of Cell Proliferation and Death. *Nature Reviews Molecular Cell Biology*, 11: 715-727, 2010.
13. F. Kocabas, J. Zheng, S. Thet, N.G. Copeland, N.A. Jenkins, R.J. DeBerardinis, C. Zhang and H.A. Sadek. Meis1 Regulates the Metabolic Phenotype and Oxidant Defense of Hematopoietic Stem Cells. *Blood*, 120: 4963-4972, 2012.
14. T. Simsek, F. Kocabas, J. Zheng, R.J. Deberardinis, A.I. Mahmoud, E.N. Olson, J.W. Schneider, C.C. Zhang and H.A. Sadek. The Distinct Metabolic Profile of Hematopoietic Stem Cells Reflects Their Location in a Hypoxic Niche. *Cell Stem Cell*, 7: 380-390, 2010.
15. A. Dahlberg, C. Delaney and I.D. Bernstein. Ex Vivo Expansion of Human Hematopoietic Stem and Progenitor Cells. *Blood*, 117: 6083-6090, 2011.
16. R. Aggarwal, J. Lu, V.J. Pompili and H. Das. Hematopoietic Stem Cells: Transcriptional Regulation, Ex Vivo Expansion and Clinical Application. *Current Molecular Medicine*, 12: 34-49, 2012.

17. E.M. Pietras, M.R. Warr and E. Passegue. Cell Cycle Regulation in Hematopoietic Stem Cells. *Journal of Cell Biology*, 195: 709-720, 2011.
18. M. Barančík, V. Boháčová, J. Kvačkajová, S. Hudecová, O.g. Križanová and A. Breier. SB203580, a Specific Inhibitor of p38-MAPK Pathway, is a New Reversal Agent of P-glycoprotein-mediated Multidrug Resistance. *European Journal of Pharmaceutical Sciences*, 14: 29-36, 2001.
19. Y. Wang, J. Kellner, L. Liu and D. Zhou. Inhibition of p38 Mitogen-activated Protein Kinase Promotes Ex Vivo Hematopoietic Stem Cell Expansion. *Stem Cells and Development*, 20: 1143-1152, 2011.
20. J. Zou, P. Zou, J. Wang, L. Li, Y. Wang, D. Zhou and L. Liu. Inhibition of p38 MAPK Activity Promotes Ex Vivo Expansion of Human Cord Blood Hematopoietic Stem Cells. *Annals of Hematology*, 91: 813-823, 2012.
21. J. Zheng, M. Umikawa, S. Zhang, H. Huynh, R. Silvany, B.P. Chen, L. Chen and C.C. Zhang. Ex Vivo Expanded Hematopoietic Stem Cells Overcome the MHC Barrier in Allogeneic Transplantation. *Cell Stem Cell*, 9: 119-130, 2011.
22. M. Oelke, M.V. Maus, D. Didiano, C.H. June, A. Mackensen and J.P. Schneck. Ex Vivo Induction and Expansion of Antigen-specific Cytotoxic T Cells by HLA-Ig-Coated Artificial Antigen-presenting Cells. *Nature Medicine*, 9: 619-624, 2003.
23. T. Nishino, C. Wang, M. Mochizuki-Kashio, M. Osawa, H. Nakauchi and A. Iwama. Ex vivo Expansion of Human Hematopoietic Stem Cells by Garcinol, a Potent Inhibitor of Histone Acetyltransferase. *PLoS One*, 6: 1-9, 2011.
24. M.A. Walasek, R. van Os and G. de Haan. Hematopoietic Stem Cell Expansion: Challenges and Opportunities. *Annals of the New York Academy of Science*, 1266: 138-150, 2012.

25. A.E. Boitano, J. Wang, R. Romeo, L.C. Bouchez, A.E. Parker, S.E. Sutton, J.R. Walker, C.A. Flaveny, G.H. Perdew, M.S. Denison, P.G. Schultz and M.P. Cooke. Aryl Hydrocarbon Receptor Antagonists Promote the Expansion of Human Hematopoietic Stem Cells. *Science*, 329: 1345-1348, 2010.
26. T. Peled, H. Shoham, D. Aschengrau, D. Yackoubov, G. Frei, G.N. Rosenheimer, B. Lerrer, H.Y. Cohen, A. Nagler, E. Fibach and A. Peled. Nicotinamide, a SIRT1 Inhibitor, Inhibits Differentiation and Facilitates Expansion of Hematopoietic Progenitor Cells with Enhanced Bone Marrow Homing and Engraftment. *Experimental Hematology*, 40: 342-355 e341, 2012.
27. K.P. Singh, R.W. Garrett, F.L. Casado and T.A. Gasiewicz. Aryl Hydrocarbon Receptor-null Allele Mice Have Hematopoietic Stem/Progenitor Cells with Abnormal Characteristics and Functions. *Stem Cells and Development*, 20: 769-784, 2011.
28. W. Li, K. Li, W. Wei and S. Ding. Chemical Approaches to Stem Cell Biology and Therapeutics. *Cell Stem Cell*, 13: 270-283, 2013.
29. S. Pelengaris, M. Khan and G. Evan. C-MYC: More Than Just a Matter of Life and Death. *Nature Reviews Cancer*, 2: 764-776, 2002.
30. B. Vennstrom, D. Sheiness, J. Zabielski and J.M. Bishop. Isolation and Characterization of C-myc, a Cellular Homolog of the Oncogene (v-myc) of Avian Myelocytomatosis Virus Strain 29. *Journal of Virology*, 42: 773-779, 1982.
31. K.S. Hatton, K. Mahon, L. Chin, F.C. Chiu, H.W. Lee, D. Peng, S.D. Morgenbesser, J. Horner and R.A. DePinho. Expression and Activity of L-Myc in Normal Mouse Development. *Molecular Cellular Biology*, 16: 1794-1804, 1996.
32. J. Charron, B.A. Malynn, P. Fisher, V. Stewart, L. Jeannotte, S.P. Goff, E.J. Robertson and F.W. Alt. Embryonic Lethality in Mice Homozygous for a Targeted Disruption of the N-myc Gene. *Genes and Development*, 6: 2248-2257, 1992.

33. B.A. Malynn, I.M. de Alboran, R.C. O'Hagan, R. Bronson, L. Davidson, R.A. DePinho and F.W. Alt. N-myc Can Functionally Replace C-myc in Murine Development, Cellular Growth, and Differentiation. *Genes and Development*, 14: 1390-1399, 2000.
34. M.J. Murphy, A. Wilson and A. Trumpp. More Than Just Proliferation: Myc Function in Stem Cells. *Trends in Cellular Biology*, 15: 128-137, 2005.
35. E. Laurenti, B. Varnum-Finney, A. Wilson, I. Ferrero, W.E. Blanco-Bose, A. Ehninger, P.S. Knoepfler, P.-F. Cheng, H.R. MacDonald, R.N. Eisenman, I.D. Bernstein and A. Trumpp. Hematopoietic Stem Cell Function and Survival Depend on C-Myc and N-Myc Activity. *Cell Stem Cell*, 3: 611-624, 2008.
36. R.N. Eisenman. Deconstructing Myc. *Genes and Development*, 15: 2023-2030, 2001.
37. C.V. Dang, K.A. O'Donnell, K.I. Zeller, T. Nguyen, R.C. Osthus and F. Li. The C-Myc Target Gene Network. *Seminars in Cancer Biology*, 16: 253-264, 2006.
38. T.-C. He, A.B. Sparks, C. Rago, H. Hermeking, L. Zawel, L.T. da Costa, P.J. Morin, B. Vogelstein and K.W. Kinzler. Identification of C-MYC as a Target of the APC Pathway. *Science*, 281: 1509-1512, 1998.
39. C.V. Dang. MYC on the Path to Cancer. *Cell*, 149: 22-35, 2012.
40. Y. Shou, M.L. Martelli, A. Gabrea, Y. Qi, L.A. Brents, A. Roschke, G. Dewald, I.R. Kirsch, P.L. Bergsagel and W.M. Kuehl. Diverse Karyotypic Abnormalities of the C-myc Locus Associated with C-myc Dysregulation and Tumor Progression in Multiple Myeloma. *Proceedings of the National Academy of Sciences of the United States of America*, 97: 228-233, 2000.

41. K. Takahashi and S. Yamanaka. Induction of Pluripotent Stem Cells from Mouse Embryonic and Adult Fibroblast Cultures by Defined Factors. *Cell*, 126: 663-676, 2006.
42. D.M. Miller, S.D. Thomas, A. Islam, D. Muench and K. Sedoris. C-Myc and Cancer Metabolism. *Clinical Cancer Research*, 18: 5546-5553, 2012.
43. H. Shim, C. Dolde, B.C. Lewis, C.S. Wu, G. Dang, R.A. Jungmann, R. Dalla-Favera and C.V. Dang. C-Myc Transactivation of LDH-A: Implications for Tumor Metabolism and Growth. *Proceedings of the National Academy of Sciences of the United States of America*, 94: 6658-6663, 1997.
44. R.C. Osthus, H. Shim, S. Kim, Q. Li, R. Reddy, M. Mukherjee, Y. Xu, D. Wonsey, L.A. Lee and C.V. Dang. Deregulation of Glucose Transporter 1 and Glycolytic Gene Expression by C-Myc. *Journal of Biological Chemistry*, 275: 21797-21800, 2000.
45. J.W. Kim, I. Tchernyshyov, G.L. Semenza and C.V. Dang. HIF-1-mediated Expression of Pyruvate Dehydrogenase Kinase: A Metabolic Switch Required for Cellular Adaptation to Hypoxia. *Cellular Metabolism*, 3: 177-185, 2006.
46. J.W. Kim, K.I. Zeller, Y. Wang, A.G. Jegga, B.J. Aronow, K.A. O'Donnell, and C.V. Dang. Evaluation of Myc E-box Phylogenetic Footprints in Glycolytic Genes by Chromatin Immunoprecipitation Assays. *Molecular Cell Biology*, 24: 5923-5936, 2004.
47. C.V. Dang, A. Le and P. Gao. MYC-induced Cancer Cell Energy Metabolism and Therapeutic Opportunities. *Clinical Cancer Research*, 15: 6479-6483, 2009.
48. M.G. Vander Heiden, L.C. Cantley and C.B. Thompson. Understanding the Warburg Effect: The Metabolic Requirements of Cell Proliferation. *Science*, 324: 1029-1033, 2009.

49. J.W. Kim and C.V. Dang. Cancer's Molecular Sweet Tooth and the Warburg Effect. *Cancer Research*, 66: 8927-8930, 2006.
50. G.L. Semenza. HIF-1 Mediates Metabolic Responses to Intratumoral Hypoxia and Oncogenic Mutations. *The Journal of Clinical Investigation*, 123: 3664-3671, 2013.
51. J.D. Gordan, J.A. Bertout, C.J. Hu, J.A. Diehl and M.C. Simon. HIF-2alpha Promotes Hypoxic Cell Proliferation by Enhancing C-myc Transcriptional Activity. *Cancer Cell*, 11: 335-347, 2007.
52. J.D. Gordan, P. Lal, V.R. Dondeti, R. Letrero, K.N. Parekh, C.E. Oquendo, R.A. Greenberg, K.T. Flaherty, W.K. Rathmell, B. Keith, M.C. Simon and K.L. Nathanson. HIF-alpha Effects on C-Myc Distinguish Two Subtypes of Sporadic VHL-deficient Clear Cell Renal Carcinoma. *Cancer Cell*, 14: 435-446, 2008.
53. C.V. Dang, J.W. Kim, P. Gao and J. Yustein. The Interplay Between MYC and HIF in Cancer. *Nature Reviews Cancer*, 8: 51-56, 2008.
54. T. Suda, K. Takubo, and G.L. Semenza. Metabolic Regulation of Hematopoietic Stem Cells in the Hypoxic Niche. *Cell Stem Cell*, 9: 298-310, 2011.
55. N. Meyer and L.Z. Penn. Reflecting on 25 Years with MYC. *Nature Reviews Cancer*, 8: 976-990, 2008.
56. J. Seoane, H.V. Le and J. Massague. Myc Suppression of the p21(Cip1) Cdk Inhibitor Influences the Outcome of the p53 Response to DNA Damage. *Nature*, 419: 729-734, 2002.
57. S. Wu, C. Cetinkaya, M.J. Munoz-Alonso, N. von der Lehr, F. Bahram, V. Beuger, M. Eilers, J. Leon and L.G. Larsson. Myc Represses Differentiation-induced p21CIP1 Expression via Miz-1-dependent Interaction with the p21 Core Promoter. *Oncogene*, 22: 351-360, 2003.

58. P. Staller, K. Peukert, A. Kiermaier, J. Seoane, J. Lukas, H. Karsunky, T. Moroy, J. Bartek, J. Massague, F. Hanel and M. Eilers. Repression of p15INK4b Expression by Myc Through Association with Miz-1. *Nature Cell Biology*, 3: 392-399, 2001.
59. T. Cheng, N. Rodrigues, H. Shen, Y. Yang, D. Dombkowski, M. Sykes and D.T. Scadden. Hematopoietic Stem Cell Quiescence Maintained by p21cip1/waf1. *Science*, 287: 1804-1808, 2000.
60. A. Wilson, M.J. Murphy, T. Oskarsson, K. Kaloulis, M.D. Bettess, G.M. Oser, A.C. Pasche, C. Knabenhans, H.R. Macdonald and A. Trumpp. c-Myc Controls the Balance Between Hematopoietic Stem Cell Self-renewal and Differentiation. *Genes and Development*, 18: 2747-2763, 2004.
61. W.Y. Langdon, A.W. Harris, S. Cory and J.M. Adams. The C-myc Oncogene Perturbs B Lymphocyte Development in E-mu-myc Transgenic Mice. *Cell*, 47: 11-18, 1986.
62. M.F. Clarke, J.F. Kukowska-Latallo, E. Westin, M. Smith and E.V. Prochownik. Constitutive Expression of a C-myb cDNA Blocks Friend Murine Erythroleukemia Cell Differentiation. *Molecular Cellular Biology*, 8: 884-892, 1988.
63. A. Gandarillas and F.M. Watt. C-Myc Promotes Differentiation of Human Epidermal Stem Cells. *Genes and Development*, 11: 2869-2882, 1997.
64. E.V. Prochownik and J. Kukowska. Deregulated Expression of C-myc by Murine Erythroleukaemia Cells Prevents Differentiation. *Nature*, 322: 848-850, 1986.
65. D.S. Askew, R.A. Ashmun, B.C. Simmons and J.L. Cleveland. Constitutive C-myc Expression in an IL-3-dependent Myeloid Cell Line Suppresses Cell Cycle Arrest and Accelerates Apoptosis. *Oncogene*, 6: 1915-1922, 1991.

66. E.A. Harrington, M.R. Bennett, A. Fanidi, and G.I. Evan. C-Myc-induced Apoptosis in Fibroblasts is Inhibited by Specific Cytokines. *EMBO Journal*, 13: 3286-3295, 1994.
67. N. Meyer, S.S. Kim and L.Z. Penn. The Oscar-worthy Role of Myc in Apoptosis. *Seminars in Cancer Biology*, 16: 275-287, 2006.
68. I.M. de Alboran, E. Baena and A.C. Martinez. C-Myc-deficient B Lymphocytes are Resistant to Spontaneous and Induced Cell Death. *Cell Death and Differentiation*, 11: 61-68, 2004.
69. E.L. Soucie, M.G. Annis, J. Sedivy, J. Filmus, B. Leber, D.W. Andrews and L.Z. Penn. Myc Potentiates Apoptosis by Stimulating Bax Activity at the Mitochondria. *Molecular Cellular Biology*, 21: 4725-4736, 2001.
70. H. Hermeking and D. Eick. Mediation of c-Myc-induced Apoptosis by p53. *Science*, 265: 2091-2093, 1994.
71. F. Zindy, C.M. Eischen, D.H. Randle, T. Kamijo, J.L. Cleveland, C.J. Sherr and M.F. Roussel. Myc Signaling via the ARF Tumor Suppressor Regulates p53-dependent Apoptosis and Immortalization. *Genes and Development*, 12: 2424-2433, 1998.
72. K. Miharada, V. Sigurdsson and S. Karlsson. Dppa5 Improves Hematopoietic Stem Cell Activity by Reducing Endoplasmic Reticulum Stress. *Cell Reports*, 7: 1381-1392, 2014.
73. A. Nogueira-Pedro, C.M. Barbosa, H.R. Segreto, L. Lungato, V. D'Almeida, A.A. Moraes, A. Miranda, E.J. Paredes-Gamero, and A.T. Ferreira. Alpha-Tocopherol Induces Hematopoietic Stem/Progenitor Cell Expansion and ERK1/2-mediated Differentiation. *Journal of Leukocyte Biology*, 90: 1111-1117, 2011.

74. S. Reykdal, C. Abboud and J. Liesveld. Effect of Nitric Oxide Production and Oxygen Tension on Progenitor Preservation in Ex Vivo Culture. *Experimental Hematology*, 27: 441-450, 1999.
75. J.P. Maciejewski, C. Selleri, T. Sato, H.J. Cho, L.K. Keefer, C.F. Nathan and N.S. Young. Nitric Oxide Suppression of Human Hematopoiesis In Vitro. Contribution to Inhibitory Action of Interferon-gamma and Tumor Necrosis Factor-alpha. *Journal of Clinical Investigation*, 96: 1085-1092, 1995.
76. B.R. Chitteti and E.F. Srour. Cell Cycle Measurement of Mouse Hematopoietic Stem/Progenitor Cells. *Methods in Molecular Biology*, 1185: 65-78, 2014.

## APPENDIX A: FLOW CYTOMETRY PLOTS AND RESULTS OF MURINE HSC

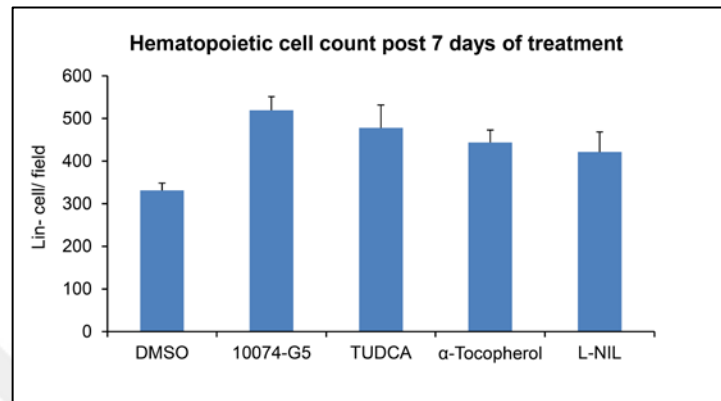


Figure A.1. Hematopoietic cell count following 7 days of HSM treatment. Cells were imaged under fluorescence microscope and analyzed by Scion image.

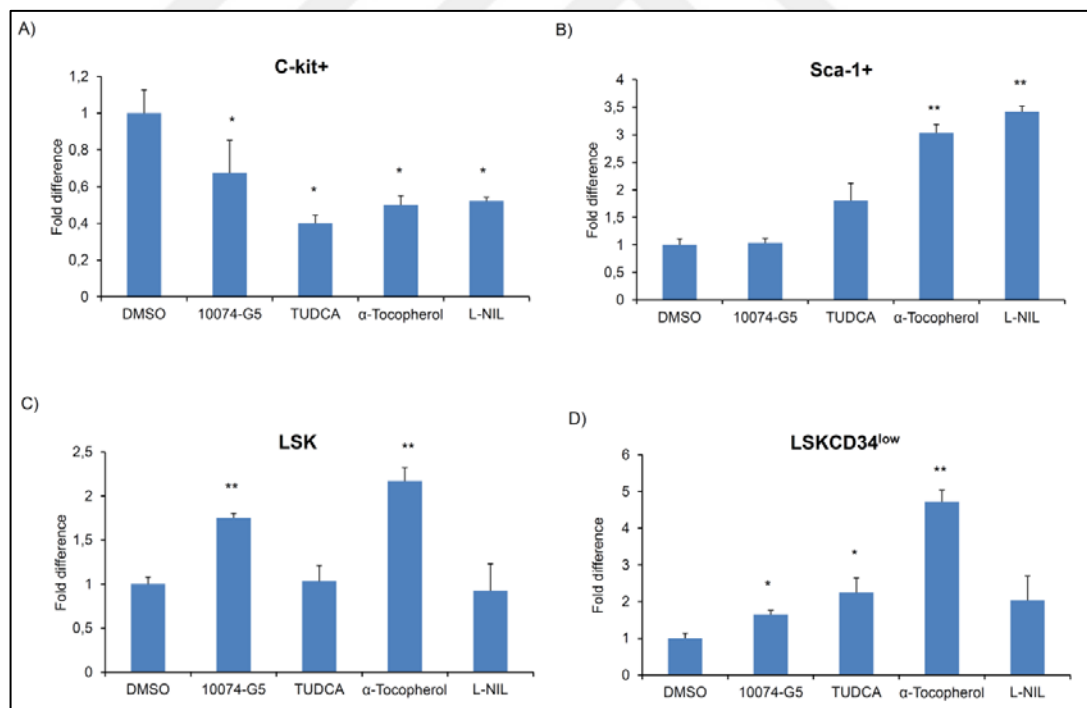


Figure A.2. Effect of C-myc inhibition on murine HSCs. Mouse lin<sup>-</sup> cells have been treated with DMSO (control, 0.5%), 10074-G5 (c-myc inhibitor, 10 μM), TUDCA (10 μM), α-Tocopherol (10 μM), L-NIL (10 μM) for 7 days and determined fold difference of A) C-Kit, B) Sca-1, C) Lin<sup>-</sup>Sca1<sup>+</sup>C-Kit<sup>+</sup> (LSK) and D) Lin<sup>-</sup>Sca1<sup>+</sup>C-Kit<sup>+</sup>CD34<sup>Low</sup> (LSKCD34<sup>low</sup>).

Note that C-myc inhibition increases LSK content. \* p < 0.05, \*\* p < 0.01. n=3.

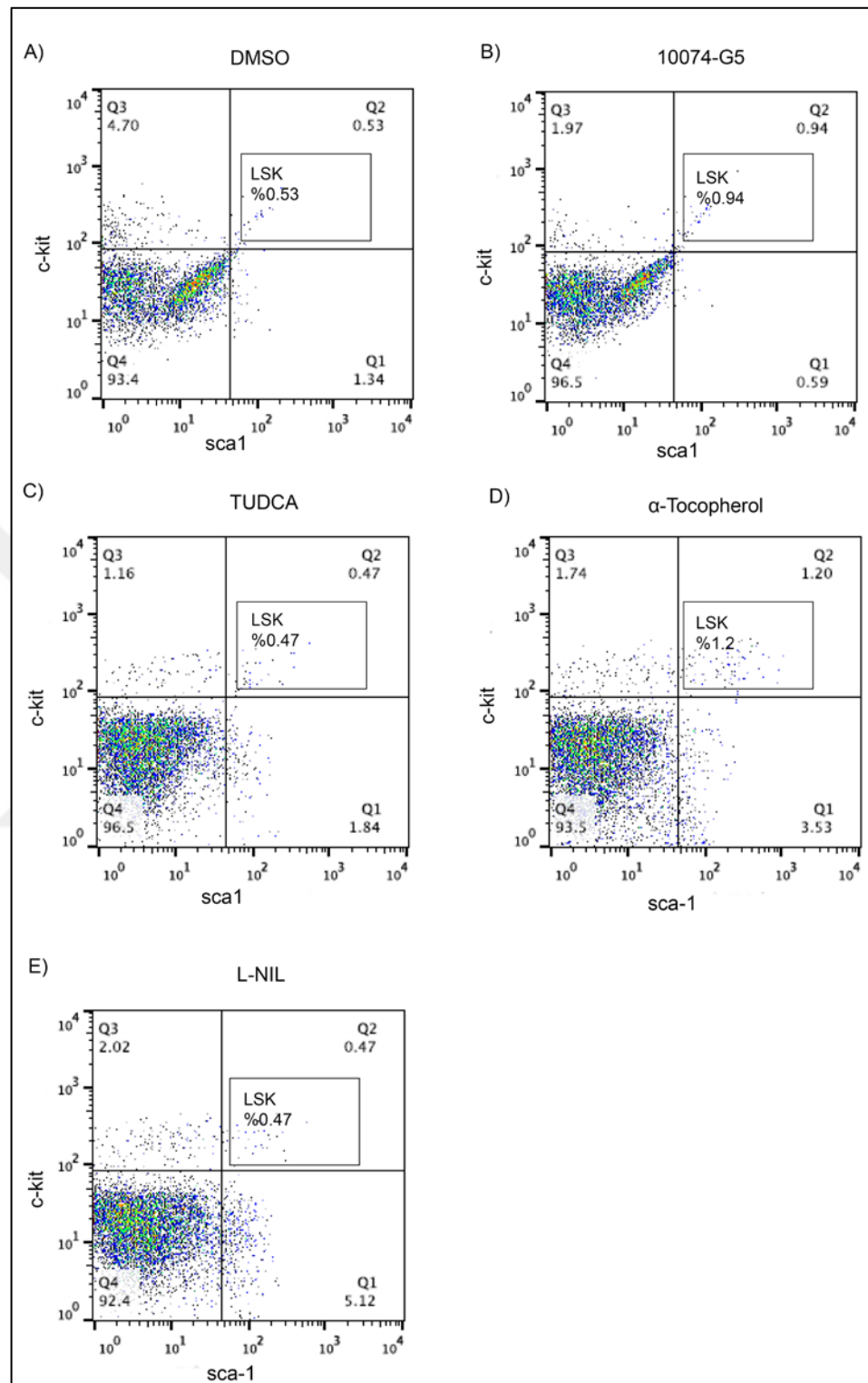


Figure A.3. Representative flow cytometry plots for murine hematopoietic stem/progenitor cells. Flow plots are referred to Lin<sup>-</sup>Sca-1<sup>-</sup>Kit<sup>+</sup> (LSK) gate of lineage negative cells that are shown for A) DMSO (control), B) 10074-G5, C) TUDCA, D)  $\alpha$ -Tocopherol and E) L-NIL.

Squares in the FACS plots indicate percentages of LSK cells in lineage negative population.

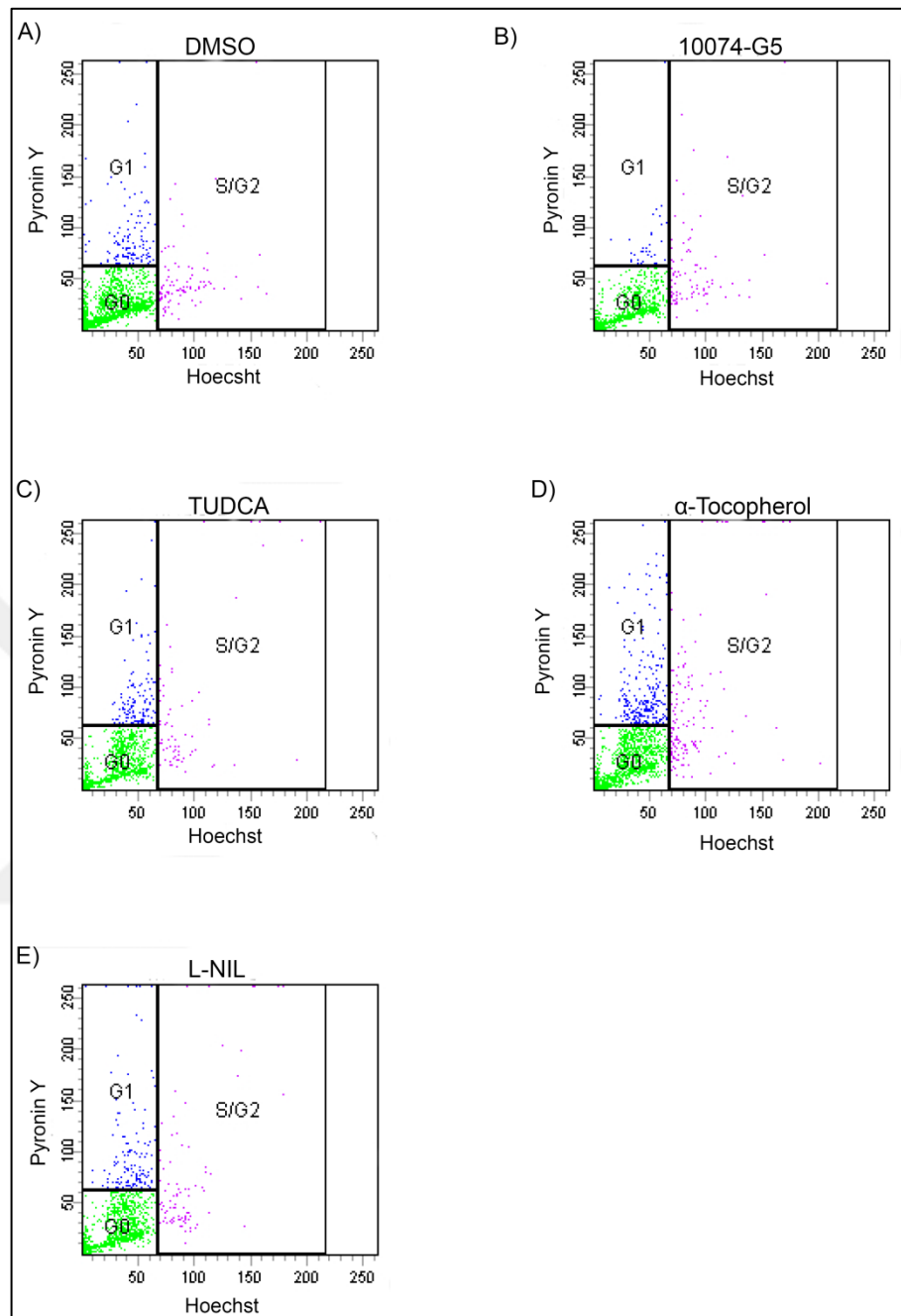


Figure A.4. Cell cycle FACS plots of murine hematopoietic stem/progenitor cells. Representative FACS analysis of Pyronin Y/Hoechst staining on HSPCs ( $\text{Lin}^- \text{Sca-1}^+ \text{Kit}^+$ , LSK) that are treated with A) DMSO (control), B) 10074-G5, C) TUDCA, D)  $\alpha$ -Tocopherol and E) L-NIL.

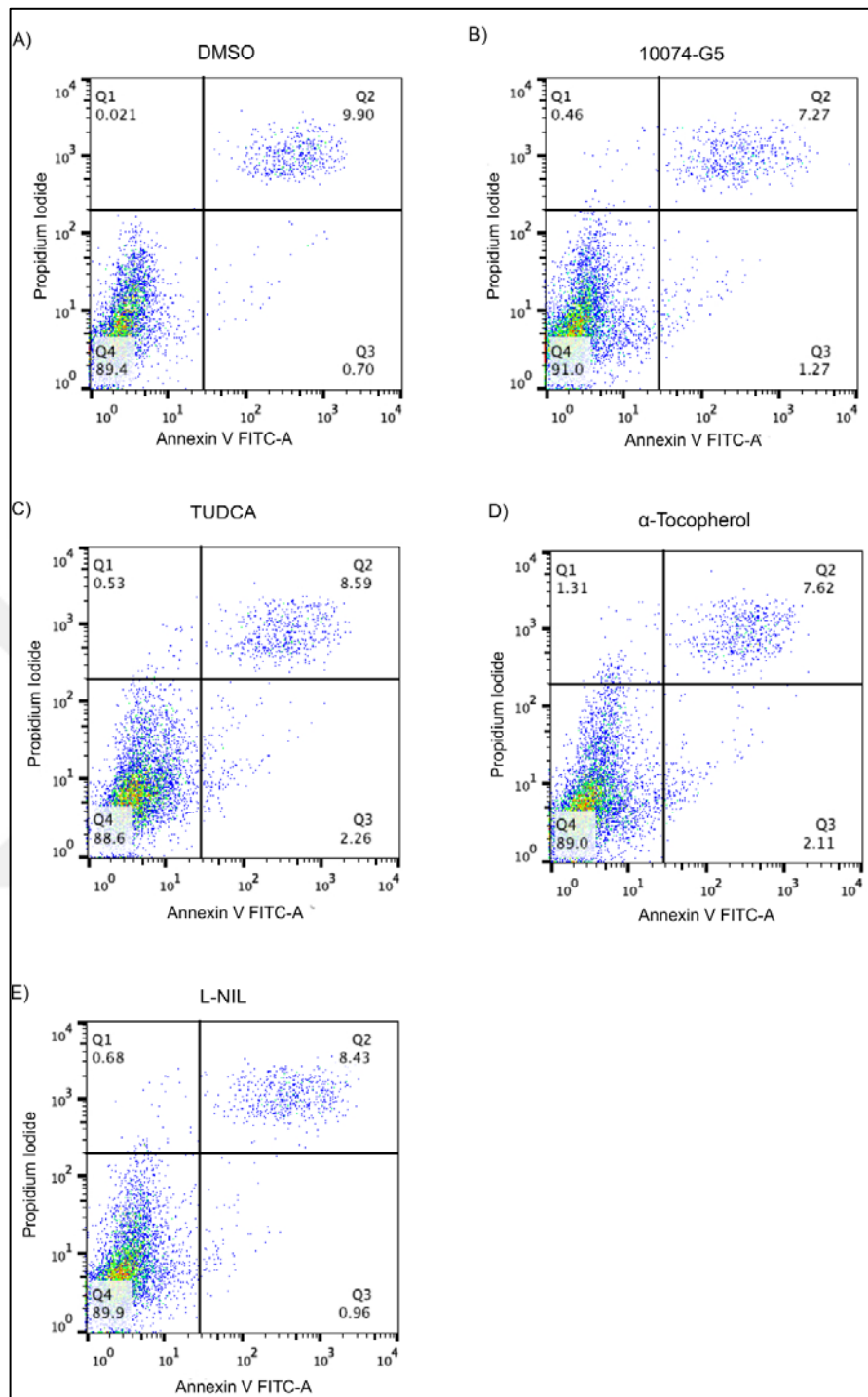


Figure A.5. Apoptosis flow plots of murine hematopoietic stem/progenitor cells. Representative Annexin V FITC-A and propidium iodide flow plots from LSK (Lin<sup>-</sup>Sca-1<sup>-</sup>Kit<sup>+</sup>) cells treated with A) DMSO (control), B) 10074-G5, C) TUDCA, D)  $\alpha$ -Tocopherol and E) L-NIL. Numbers in the FACS plots indicate percentages (Q1; necrotic, Q2; late-apoptotic, Q3; early-apoptotic, Q4; live cells) among LSK cells.